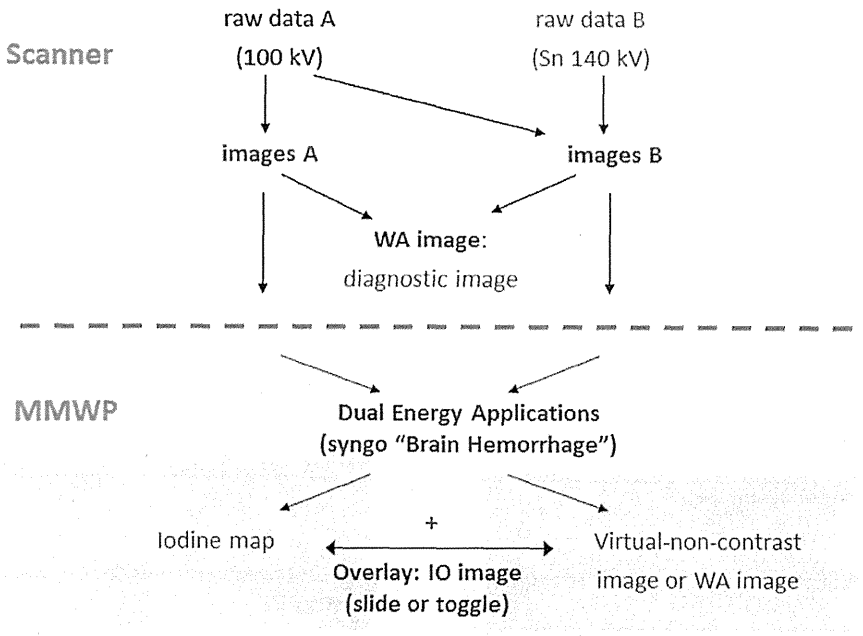

Fig. 1. Flow chart showing an overview of post-processing. Weighted-average (WA) CT images are generated by fusing data sets acquired with different tube voltages (100 and 140 kV). WA images resemble conventional CT images. Iodine overlay (IO) images are generated by fusing virtual non-contrast images and iodine images at a ratio of 0.5.

15; field of view, 230 mm; matrix, 224 × 224; slice thickness/gap, 1.0 mm/0 mm) and fat saturated contrast-enhanced (TR/TE, 6/1.15; flip angle, 15; field of view, 230 mm; matrix, 224 × 224; slice thickness/gap, 1.0 mm/0 mm). Images in the coronal or sagittal plane may be obtained in order to evaluate certain anatomic spaces, such as the preepiglottic space in the sagittal plane, or the paraglottic space and the ventricle in the coronal plane.

3.3. Dual-energy CT

3.3.1. Basic principles

Single-energy CT generates images based on the X-ray absorption coefficient of scanned tissues, and according to their density the tissues are assigned a CT value and displayed as a grey scale. As a result, it may be difficult to differentiate materials of different chemical composition, such as iodine and bone or iodine-enhanced lesions and cartilage, as they have the same CT value on CT images [8,26]. This difficulty can be overcome for some materials using dual-energy CT [15,27,28] which exploits the dependence of the absorption coefficient on the energy of the X-ray spectrum, or kV setting, used for the scan [13,29–31]. For example, materials such as iodine have lower CT values at high X-ray energies than at low X-ray energies, whereas fat tissue shows the opposite behavior. The CT value of water, soft tissue and blood stays almost constant at all X-ray energies.

In practice, two CT images taken at different tube voltages, typically 80 or 100 kV and 140 kV, are sufficient to classify many tissues. Different scan techniques have been developed to acquire dual-energy CT data sets; dual-source dual-energy CT, dual-energy CT with fast kilovolt switching, and multilayered-detector dual-energy CT [32,33]. Here, we limit our discussion to dual-source dual-energy CT [33,34], used at our institution.

Several algorithms can be used to extract material information and generate material maps or remove materials from images. A three-material decomposition algorithm applied to each voxel of an iodine-enhanced dual-energy CT image set makes it possible to compute iodine maps and virtual non-contrast images. Three materials have to be predefined for this algorithm according to the scanned body area: for example iodine, soft tissue and air are chosen for lung imaging [14], and iodine, fat and tissue for liver imaging [33]. For the head-neck region, the materials are set to iodine, brain parenchyma and hemorrhage [12,16].

3.3.2. Dual-energy CT protocol

For dual-source dual-energy CT scans using 128-slice dual-source CT (SOMATOM Definition Flash; Siemens Healthcare, Forchheim, Germany), the following parameters are applied: 100 and 140 kV tube voltages with a 0.4-mm tin filter (labeled as Sn140 kV), 200 and 200 effective mAs, 0.33-s rotation time, 32 × 0.6-mm collimation with a z-flying focal spot, and a pitch of 0.6. The tin filter blocks low-energy X-rays from the 140 kV spectrum, thus reducing radiation to the patient and enhancing energy separation of X-rays from the low and high kV X-ray tubes. These parameters result in an average CT dose index of 14–15 mGy, which is equivalent to that of single-energy CT scans. Noise needs to be minimized to ensure precise three-material decomposition in the head and neck, where many heterogeneous structures such as cartilage, soft tissues and air in the trachea require a high image resolution. A voltage combination of 100 kV and Sn140 kV, rather than 80 and 140 kV, is chosen to minimize noise while maximizing the separation of the X-ray tubes' energy spectra. The methods of contrast material injection are the same as for conventional CT.

3.3.3. Image reconstruction and post-processing

The image reconstruction and post-processing flow is shown in Fig. 1: two sets of raw data (100 kV and Sn140 kV) are separately reconstructed from the acquired dual-energy data using a 1-mm slice thickness and 0.7-mm increment, and a third, WA image set is generated at the same time, linearly weighing and fusing each pixel of the 100-kV and Sn140 kV data (p100 and p140, respectively) at the default ratio of $w = 0.5$ according to the following formula: $[w \times \text{p100}] + [(1 - w) \times \text{p140}]$. A medium sharp D30f kernel is applied for all reconstructions. WA images are used as diagnostic images since they are equivalent in terms of image quality to single-energy 120 kV CT images [35,36].

Next, the images are post-processed on a separate workstation (MMWP; Siemens Healthcare), and three-material-decomposition analysis (Syngo Dual Energy, Brain Hemorrhage; Siemens

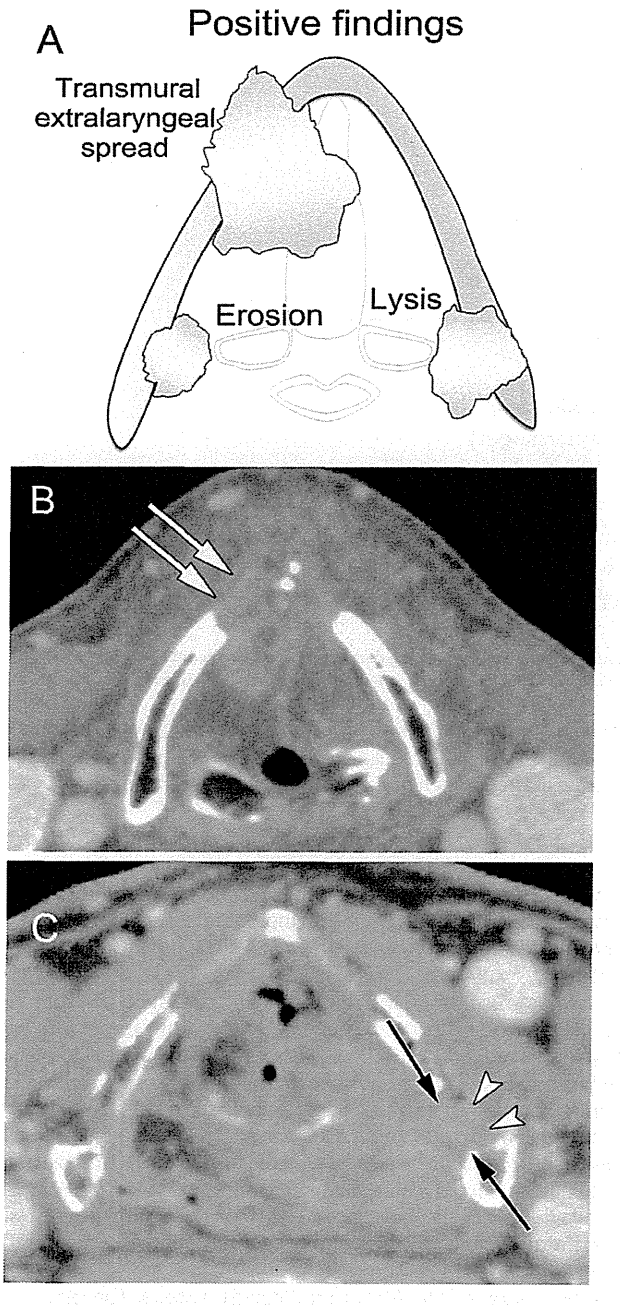

Fig. 2. (A) Drawing to illustrate the criteria for evaluation of thyroid cartilage invasion. Erosion is defined as invasion beyond the inner cortex without reaching the outer cortex (less than half of the cartilage width), lysis is defined as almost reaching the outer cortex but with preservation of the cortex, and extralaryngeal spread is defined as all-layer invasion through both the inner and outer cortex (penetration) of the cartilage, including the extralaryngeal soft tissues. (B) Positive finding of invasion through the outer cortex of the thyroid cartilage in a 56-year-old man with glottic cancer. Axial contrast-enhanced CT image at the level of the vocal cords shows tumor invasion into the thyroid cartilage, spreading into the extralaryngeal soft tissue (white arrows). (C) Positive finding of thyroid cartilage lysis in a 69-year-old man with hypopharyngeal cancer. Axial contrast-enhanced CT image at the glottic level shows a tumor mass arising from the left piriform sinus. The inner cortex of the left thyroid cartilage shows disappearance of a thin hypo-attenuated line between the tumor and the cartilage (arrows), and substitution of cartilage with tumor tissue as demonstrated by CT attenuation (arrowheads).

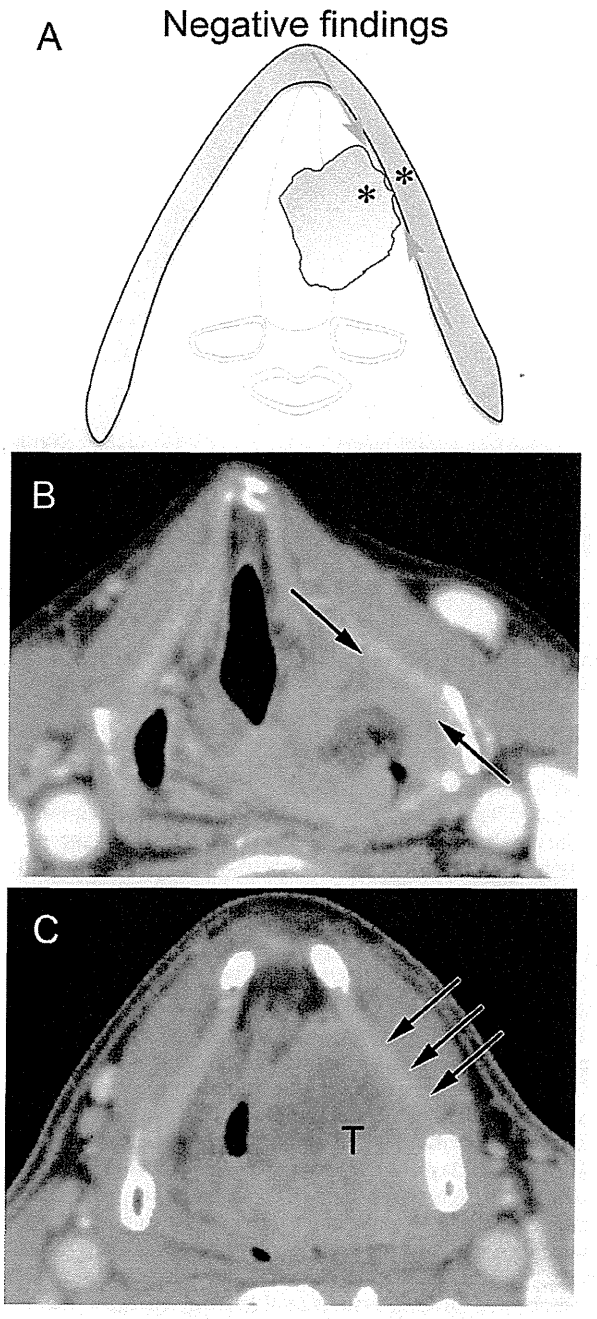

Fig. 3. (A) Drawing to illustrate the criteria for negative thyroid cartilage invasion based on two concurrent findings: (1) perfect or almost continuously defined thin hypo-attenuated line between the tumor and the cartilage (arrows), (2) difference in CT attenuation between non-ossifying cartilage and the tumor (asterisks). (B) Negative finding of thyroid cartilage invasion in a 67-year-old man with hypopharyngeal cancer. Axial contrast-enhanced CT image at the level of the false vocal cords shows a tumor mass arising from the left piriform sinus, but preservation of a dark line between the tumor and the cartilage is evident (arrows). (C) Negative finding of thyroid cartilage invasion in a 61-year-old man with hypopharyngeal cancer. Axial contrast-enhanced CT image at the supraglottic level shows a tumor mass arising from the left piriform sinus. CT attenuation of the non-ossifying cartilage (arrows) is different from that of the tumor (T).

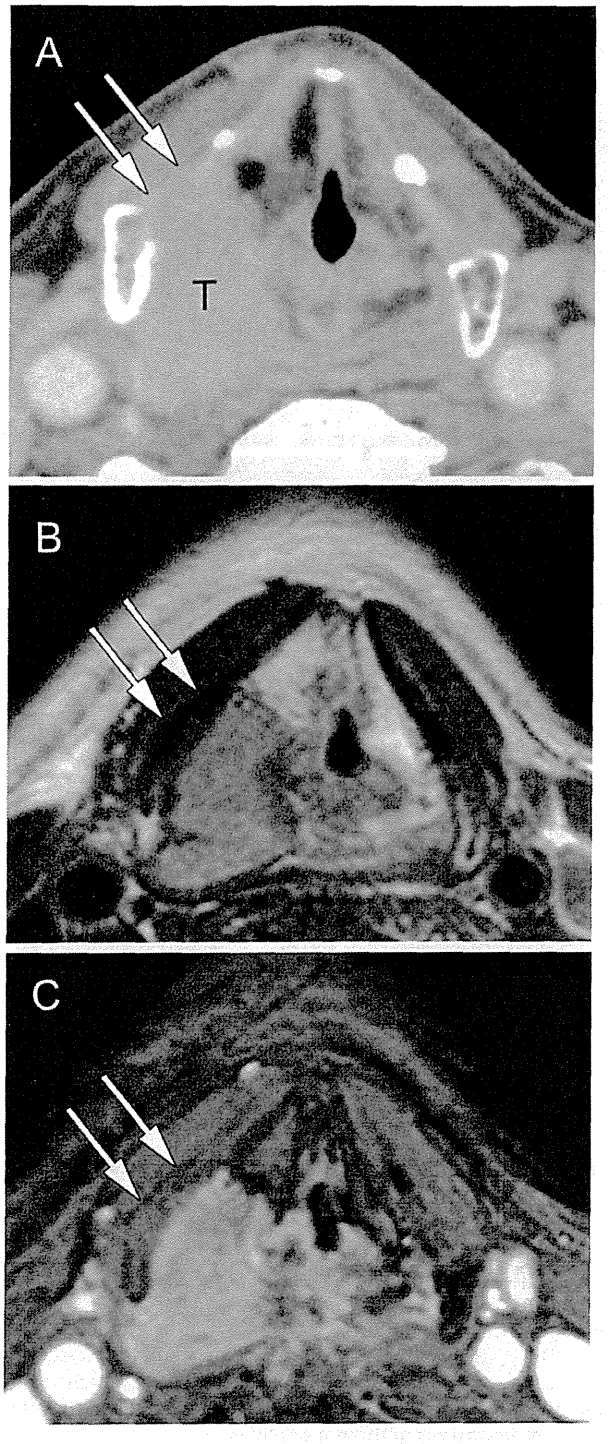

Fig. 4. True negative finding for thyroid cartilage invasion by MR imaging in a 69-year-old man with hypopharyngeal cancer. (A) Axial contrast-enhanced CT image at the level of the false vocal cords shows tumor mass (T) arising from the right piriform sinus. The tumor is located adjacent to non-ossified cartilage of the right thyroid lamina, and the tumor and cartilage show similar CT values, making them almost indistinguishable (arrows). (B) T2-weighted MR image obtained at the same level shows a right-sided piriform sinus tumor with intermediate signal intensity. The adjacent right thyroid lamina can be differentiated by its low signal intensity (arrows). (C) Fat-suppressed contrast-enhanced T1-weighted image shows contrast enhancement of the tumor mass and poor enhancement of the thyroid lamina (arrows) relative to the adjacent tumor mass. Pathological findings confirmed that there was no tumor cell infiltration into the cartilage.

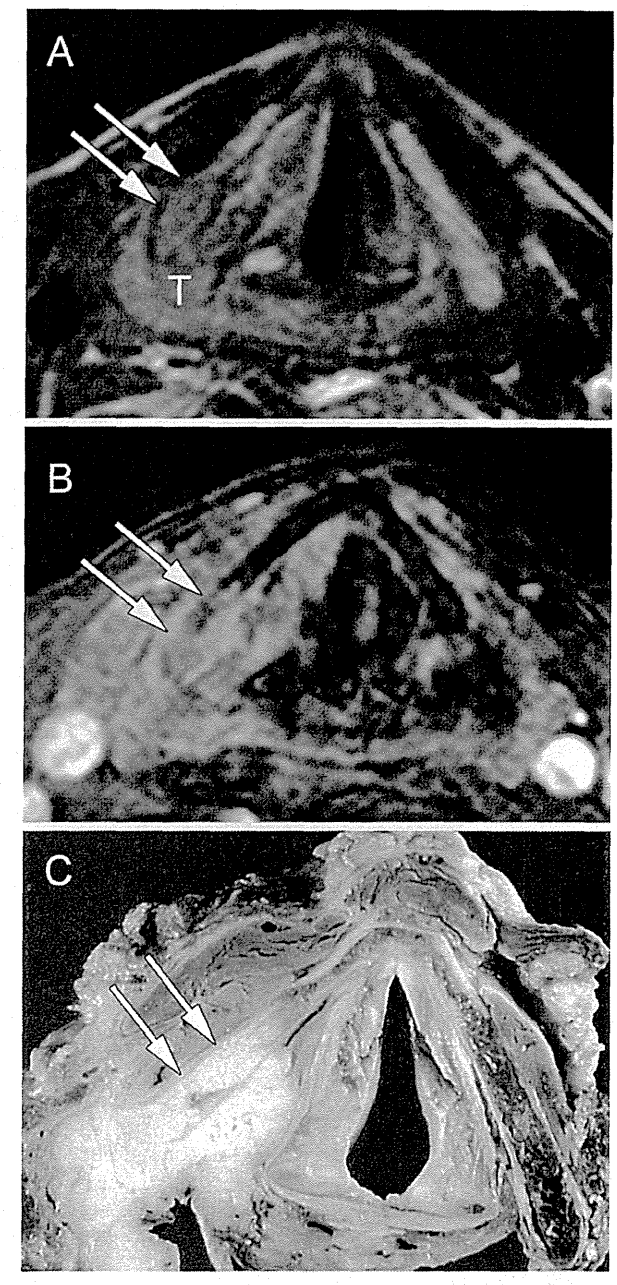

Fig. 5. Positive finding of thyroid cartilage invasion on MR imaging in a 69-year-old man with hypopharyngeal cancer. (A) Axial T2-weighted image at the level of the vocal cords shows a tumor mass (T) arising from the right piriform sinus with intermediate signal intensity. The adjacent right thyroid cartilage shows a similar signal intensity (arrows). (B) Fat-suppressed contrast-enhanced T1-weighted image shows enhancement of the tumor mass and similar enhancement of the adjacent thyroid lamina (arrows). (C) Corresponding axial slice from the surgical specimen at the same level confirms that the posterior thyroid cartilage has been invaded by the tumor cells (arrows).

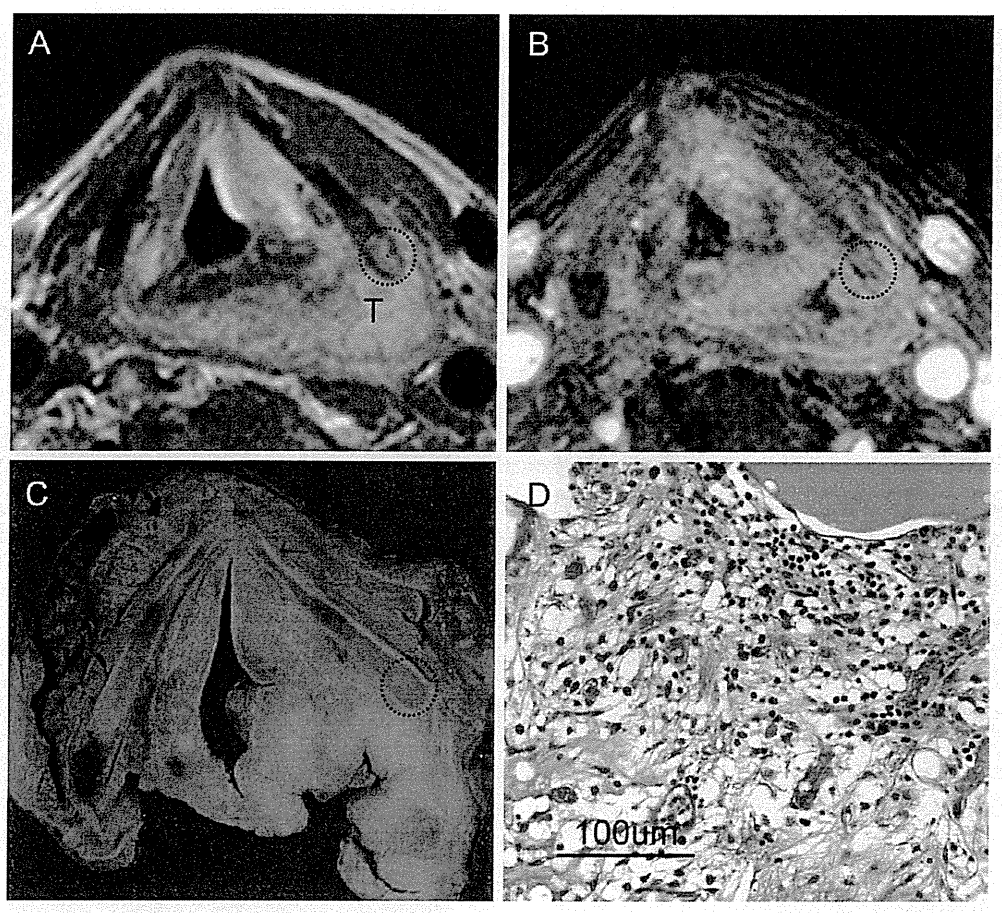

Fig. 6. False-positive findings for thyroid cartilage invasion by MR imaging in a 59-year-old man with hypopharyngeal cancer. (A) T2-weighted MR image at the glottic level shows a tumor mass (T) arising from the left piriform sinus with invasion of the paraglottic space and extension into the soft tissues of the neck. The tumor shows intermediate signal intensity, and the adjacent thyroid cartilage has similar signal intensity (circle). (B) Fat-suppressed contrast-enhanced T1-weighted image shows enhancement of the tumor mass and similar enhancement of the adjacent thyroid lamina (circle). (C) Corresponding axial slice from the surgical specimen at the same level shows that the left thyroid lamina has not been invaded by the tumor (circle). (D) Posterior part of the left thyroid lamina with enhancement (circle in B) shows the moderate infiltration of lymphocytes into the medullary space, accompanied with fibrosis and aggregation of macrophages. (Hematoxylin–eosin stain; original magnification 200×.).

Healthcare) is used to compute iodine images and virtual non-contrast images. The algorithm can be applied at the default parameters for extracting iodine since pharyngeal and laryngeal soft tissues and cartilages have CT values similar to hemorrhage and brain parenchyma. "Organ contour enhancement" and "resolution enhancement" are deselected to ensure quantitative analysis of the small cartilage structures. Finally, the iodine images and the virtual non-contrast or weighted average (WA) images can be linearly fused at a ratio of 0.5, creating iodine overlay (IO) images.

Reconstructed images can then be generated from the WA images and the IO images as frontal and coronal sections parallel and vertical to the vocal cords from 1 cm above the hyoid bone to the inferior margin of the cricoid cartilage (2-mm thickness and 16-cm field of view).

4. Clinical application of CT, MR imaging and dual-energy CT

4.1. Cartilage invasion

Both CT and MR imaging are routinely used for detection of subtle cartilage invasion, but there is still controversy about which modality can most accurately detect cartilage invasion, and both modalities have shortcomings [8,26,37,38]. Dual-energy CT may have the potential to overcome some of the shortcomings of conventional CT, due to the possibility of iodine contrast becoming distributed in tumor tissues but not in normal cartilage. Iodine enhancement can reveal the presence and shape of a tumor, and combined analysis of WA and IO images can be applied to evaluate cartilage invasion. In the next few paragraphs, we discuss the appearances of laryngeal cartilage invasion with conventional CT and MR imaging, as well as dual-energy CT, and explain the advantages and limitations of these modalities.

4.1.1. Conventional CT

Previous studies using single-slice spiral CT scanners have concluded that the CT criteria used for determining neoplastic invasion of the thyroid cartilage include erosion, lysis, and transmural extralaryngeal tumor spread [17,18,26,38,39]. These positive signs of invasion are defined according to the depth of invasion into cartilage, and careful evaluation of the shape and attenuation of the thyroid cartilage (Fig. 2A). In 1997, Becker et al. redefined the diagnostic criteria for single-slice CT and were able to reach an acceptable balance of 71% sensitivity versus 83% specificity by applying these criteria [26]. For evaluation of extralaryngeal spread

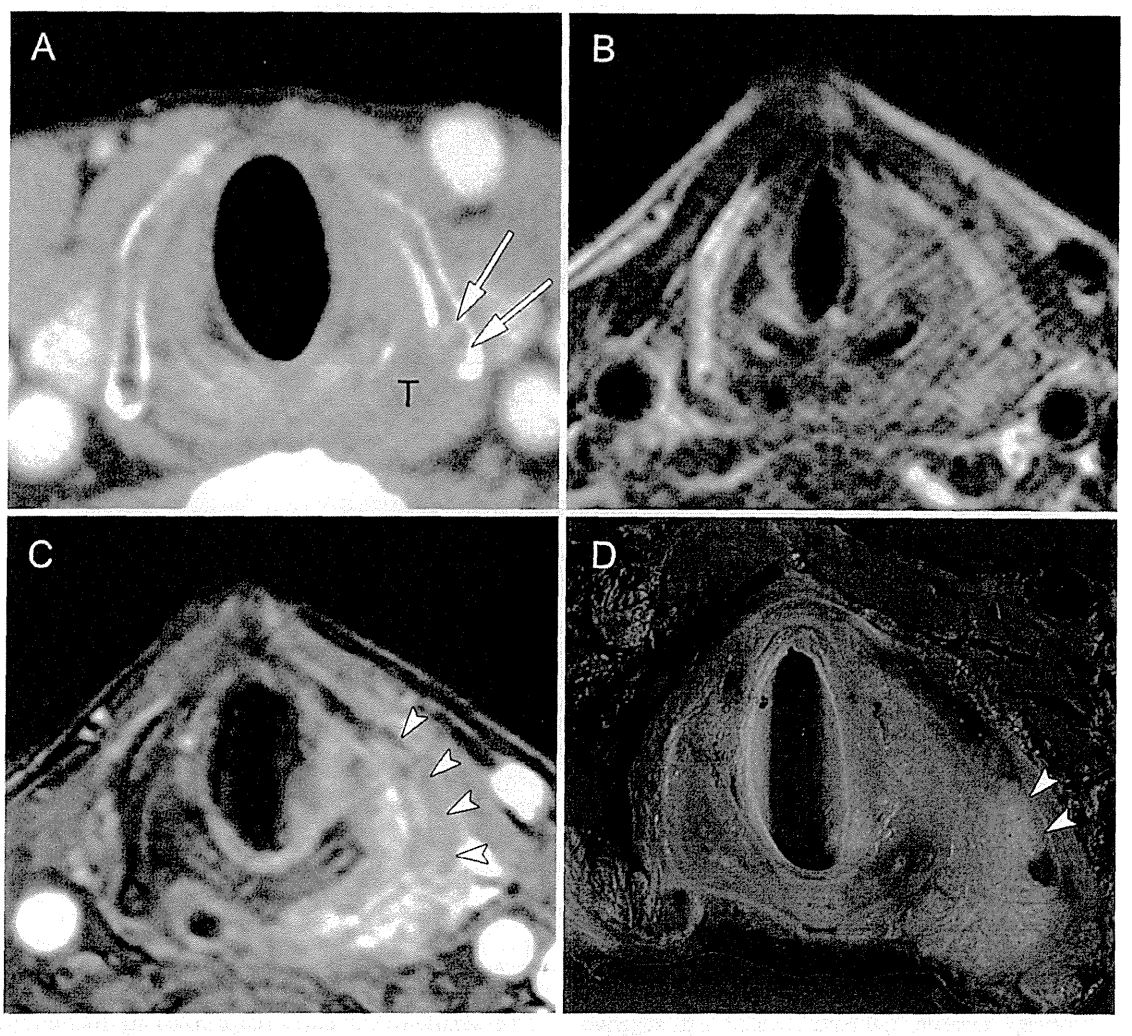

Fig. 7. Hypopharyngeal cancer in a 67-year-old man with thyroid cartilage invasion. (A) Axial contrast-enhanced CT image at the subglottic level shows a tumor mass (T) arising from the right piriform sinus with evidence of focal lysis on the left thyroid cartilage (arrows). (B) T2-weighted MR image obtained at the same level shows a left-sided piriform sinus tumor with intermediate signal intensity. As the motion artifacts are strong, no anatomical information can be obtained in that area and tumor invasion cannot be identified. (C) Fat-suppressed contrast-enhanced T1-weighted image shows more extensive contrast enhancement of the tumor mass and thyroid cartilage than the CT findings. (D) A corresponding slice of the surgical specimen shows the focal infiltration of the tumor into cartilage (arrowheads), consistent with the findings of CT imaging. Thus, the range of tumor cell invasion was overestimated on the fat-suppressed contrast-enhanced T1-weighted MR image.

with cartilage invasion, CT may easily identify tumor growth outside the larynx with cartilage invasion to the soft tissues of the neck (Fig. 2C). This finding is the most reliable criterion of invasion, but is evident only in advanced cases. When determining whether erosion or lysis is present or absent, differentiation from cartilage invasion may sometimes be difficult using conventional CT (Fig. 2B). Some cases may be distinguished from erosion if two concurrent findings of negativity are identified (Fig. 3A): a perfect or almost continuously defined thin hypo-attenuating line between the tumor and the cartilage (Fig. 3B), and CT attenuation of non-ossifying cartilage that differs from that of the tumor (Fig. 3C). However, distortion of adjacent normal structures may mimic tumor involvement, even with careful evaluation.

Asymmetrical sclerosis, defined as thickening of the cortical margin, increased medullary density, or both, when comparing one arytenoid with the other, or one side of the cricoid or thyroid cartilage with the other side, is a sensitive but non-specific feature of cartilage invasion on CT [26,40–42]. For the thyroid cartilage, asymmetric sclerotic changes (ossification) without erosion or lysis should not be diagnosed as positive, as these changes sometimes represent reactive inflammatory changes [26].

The introduction of multi-slice CT has resulted in an increase of spatial and temporal resolution but has led to little progress in interpretation of cartilage invasion [43], which is still sometimes overestimated [9,10]. A fundamental problem of CT is that laryngeal non-ossified cartilage and tumors show similar CT values of about 100 HU, making them almost indistinguishable, especially when the tumor is located adjacent to non-ossified cartilage (Fig. 4A) [8,26]. In addition, the appearance of laryngeal cartilage on CT varies widely according to differences in the proportions of hyaline cartilage (which ossifies with aging), cortical bone, and fatty marrow, which complicates interpretation.

4.1.2. MR imaging

MR imaging seems to be more sensitive than CT for detecting thyroid cartilage invasion (sensitivity up to 96%), as the high contrast resolution of MR makes it possible to detect small areas of marrow space invasion [18,38,44,45]. When assessing cartilage invasion with MR imaging, the T2-weighted and contrast-enhanced T1-weighted signal intensities of the cartilage should be compared with the signal intensities of the adjacent tumor [45]. If the cartilage displays a signal intensity similar to that of the tumor, cartilage

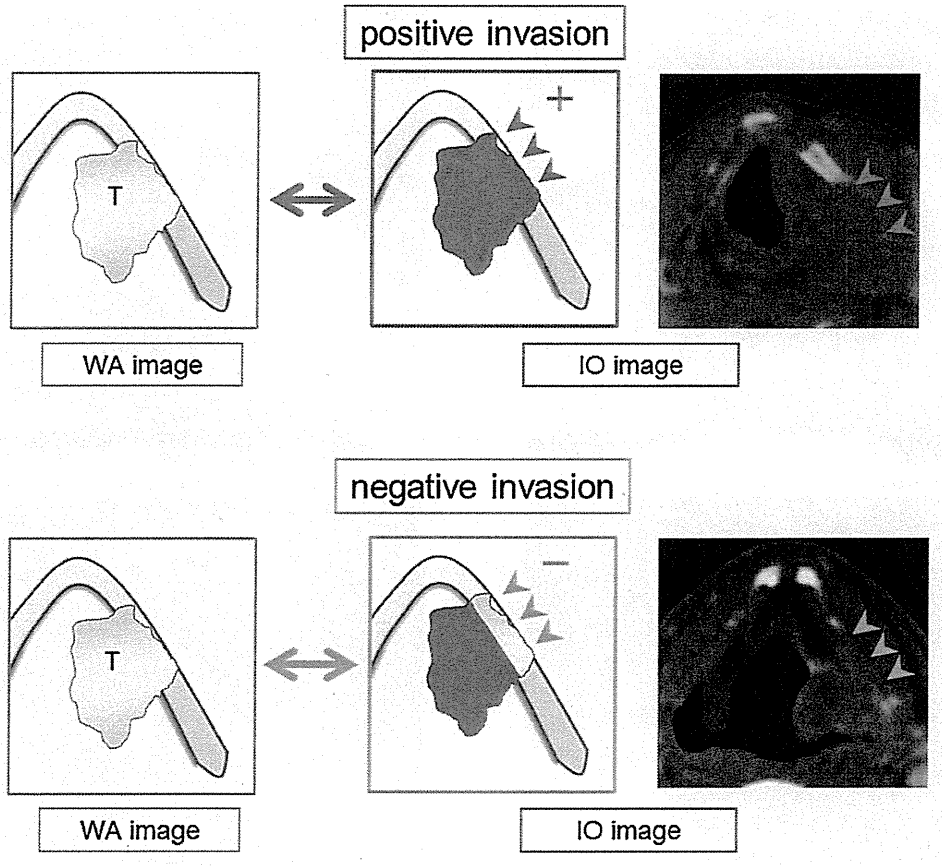

Fig. 8. Criteria for evaluation of cartilage invasion on dual-energy CT WA and IO images.

invasion should be suspected (Fig. 5). Contrast-enhanced MR imaging is also useful when evaluations by CT alone are insufficient for excluding cartilage invasion, and have reached high negative predictive values of up to 96% (Fig. 4) [38,45].

However, the MR findings suggestive of cartilage invasion are not specific, and therefore may lead to a number of false positive signs. The reason is that reactive inflammation, edema and fibrosis in the vicinity of a tumor may demonstrate diagnostic features similar to those of cartilage invasion (Fig. 6). Inflammatory changes are most common in the thyroid cartilage, and therefore the specificity of MR imaging for detecting invasion of the thyroid cartilage is only 56–65% [38,45]. Furthermore, MR resolution is often degraded by motion artifacts [45] and lacks thin sections (Fig. 7B), and the area of tumor extension into cartilage is more easily overestimated on MR imaging than on CT (Fig. 7C). Both of these factors mean that MR imaging is not a satisfactory first choice for imaging of laryngeal and hypopharyngeal cancer.

4.1.3. Dual-energy CT

The recommended dual-energy CT criteria for laryngeal cartilage invasion are summarized in Fig. 8. The IO images are read in addition to the WA images to identify the iodine distribution corresponding to the area displayed on the WA images. After a lesion has been evaluated as positive on WA images, the iodine distribution on the IO images is examined to derive a final classification of either positive or negative. When the IO image shows a corresponding area of tumor cartilage invasion as a red-colored area, positive invasion can be considered based on the combined findings evident on WA and IO images (Fig. 9). When the IO image does not show a corresponding area of tumor cartilage invasion as a red-colored area, tumor invasion can be defined as negative (Fig. 10).

A preliminary report suggests that dual-energy CT has the potential to increase diagnostic performance and reproducibility for evaluation of thyroid cartilage invasion [16]. The reported specificity of combined analysis of WA and IO images obtained with dual-energy CT is significantly superior to that of WA imaging alone (96% vs. 70%) with no compromise of sensitivity (86% vs. 86%), and the interobserver reproducibility of diagnosis using a combination of WA plus IO images is higher than that with WA imaging alone (especially for evaluation of thyroid and cricoid cartilage invasion) [16], and also that reported in a few studies using single-section spiral CT [46,47].

When interpreting the findings of dual-energy CT, it is important to be aware of certain technical limitations. Since this technique applies a 3-material decomposition algorithm with soft tissues and iodine as predefined materials [12,13,33], bone and calcified structures are classified into iodine or soft tissues according to tissue density, and cannot be clearly identified on IO images. As a result, lesions that include calcified structures such as sclerosis and previously ossified parts of cartilage need to be evaluated on WA images first, because on IO images iodine distribution may be overestimated. This does not create an advantage or disadvantage compared to conventional CT, since WA images already have image quality similar to that of conventional CT images. In short, diagnostic reading should always start with the WA image, followed by additional reading of the IO image when appropriate [16].

4.2. Extralaryngeal tumor spread

Extralaryngeal tumor spread is considered to be present when the primary tumor has expanded into extralaryngeal soft tissues, such as cervical soft tissues, the infrahyoid muscles, thyroid gland,

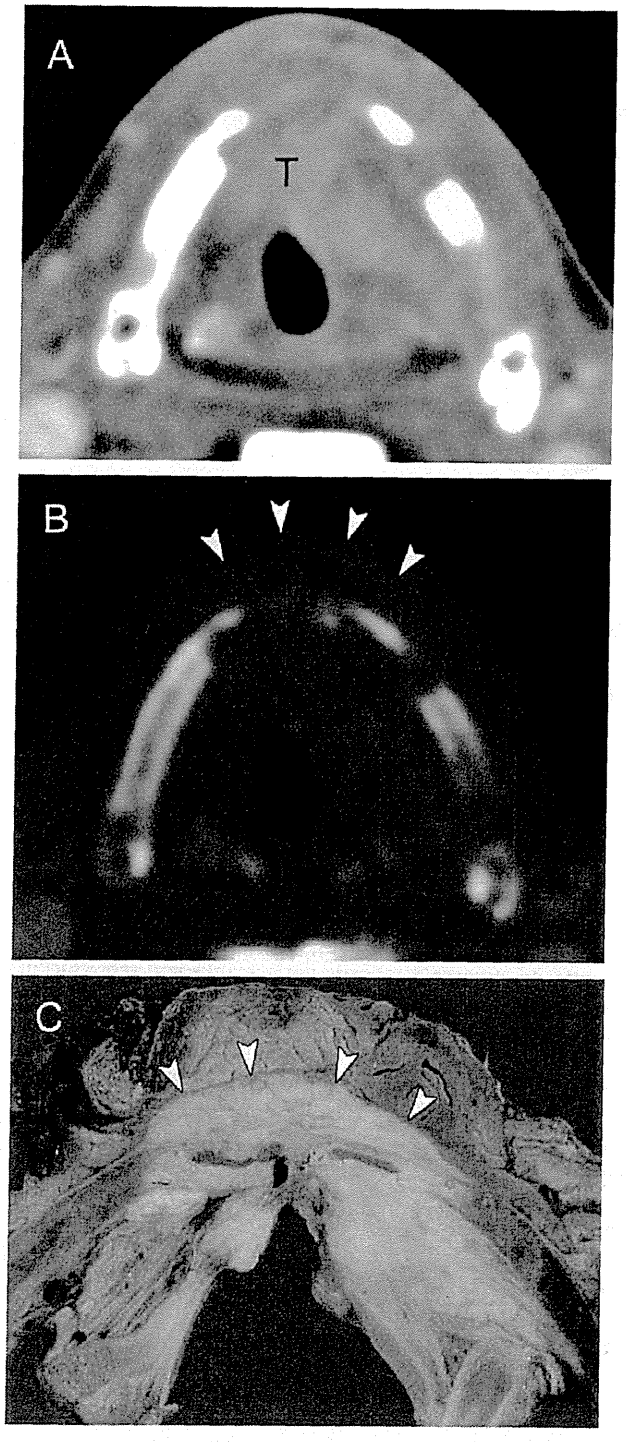

Fig. 9. Positive finding of thyroid cartilage invasion through the outer cortex by dual-energy CT in a 60-year-old man with supraglottic cancer. (A) WA image at the glottic level shows tumor (T) invasion into the thyroid cartilage, spreading into the extralaryngeal soft tissue. (B) On the IO image, the extent of extralaryngeal tumor spread is clearly evident (arrowheads). (C) A corresponding slice of the surgical specimen shows the tumor cell penetrates through the cartilage and invades the extralaryngeal soft tissue (arrowheads), consistent with the findings of the IO image.

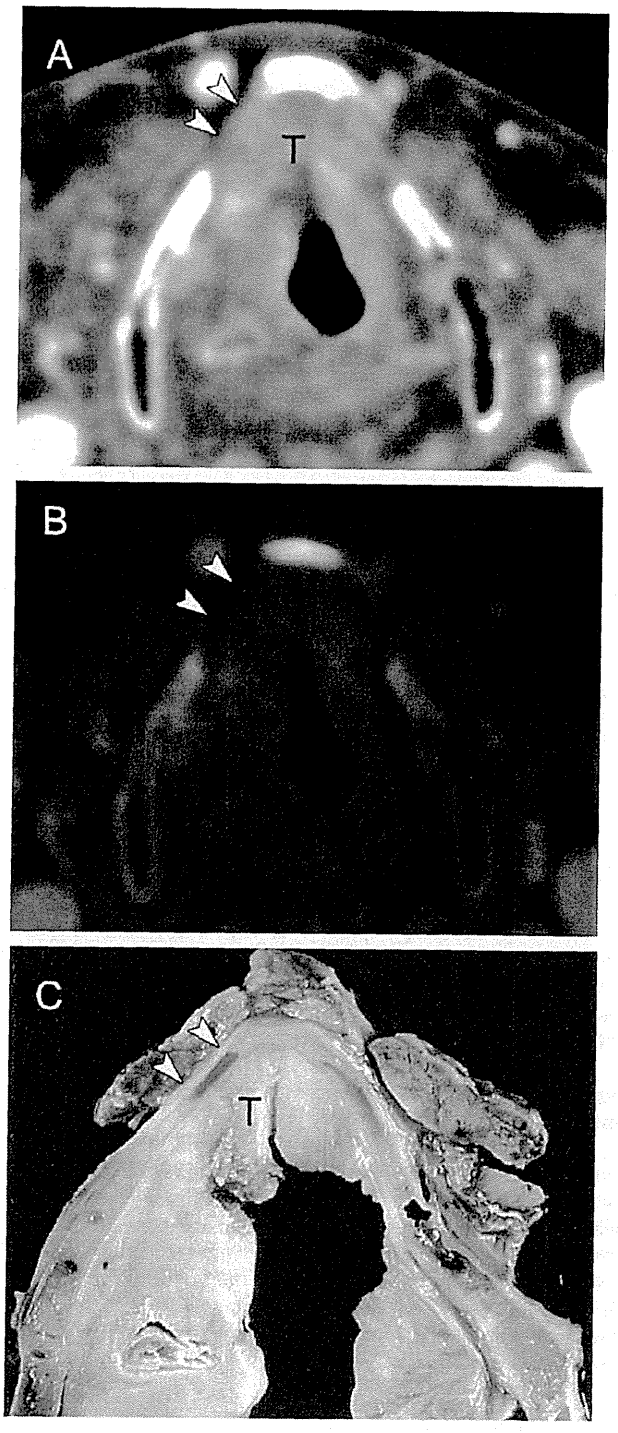

Fig. 10. Negative finding for erosion in the thyroid cartilage by dual-energy CT in a 68-year-old man with glottic cancer. (A) WA image at the level of the vocal cords shows a tumor mass (T) that has invaded the paraglottic space. Non-ossified cartilage of the right thyroid lamina has been substituted by the tumor (arrowheads). (B) IO image clearly shows no corresponding enhancement of the thyroid cartilage (arrowheads). (C) The corresponding slice of the surgical specimen shows that the right thyroid cartilage has not been invaded by the tumor cells (arrowheads).

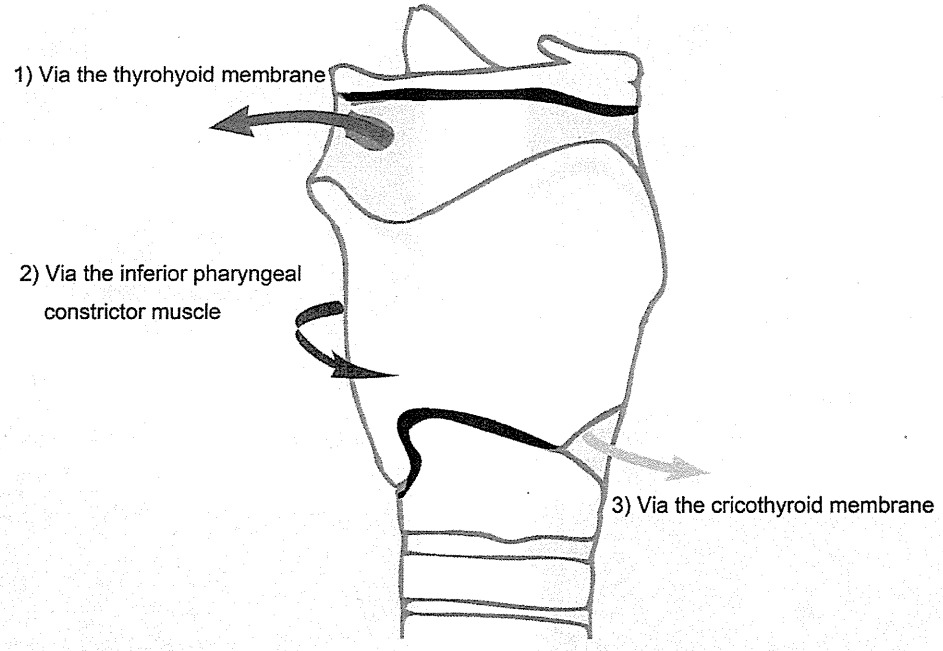

Fig. 11. Drawings (right lateral view of laryngeal box) illustrate the routes of tumor spread out from the larynx through areas of inherent weakness; (1) via the thyrohyoid membrane along the superior laryngeal neurovascular bundle (red arrow), (2) via the inferior pharyngeal constrictor muscle (blue arrow), (3) via the cricothyroid membrane (yellow arrow).

esophagus, trachea, or deep lingual muscle, with or without cartilage penetration [20]. In clinical practice, patients with T4 disease do not always inevitably undergo laryngectomy, and for patients without tumor extension through the cartilage – a diagnosis that is not always straightforward – clinicians rely on imaging for accurate tumor staging, tumor mapping and detection of possible tumor extension [5,6]. It is then possible to predict which patients may be candidates for function-preserving treatments to some degree, and discussions with the patients are part of the treatment decision process.

According to Beitler et al. [39], extralaryngeal spread without thyroid cartilage penetration was more common than previously expected in patients with advanced laryngeal and hypopharyngeal cancer. The authors suggested that cartilage invasion was absent in 40% of cases showing extralaryngeal tumor spread. Since extralaryngeal tumor spread is one of the important predictors of T4 disease in laryngeal and hypopharyngeal cancer, the focus of imaging needs to shift from detection of invasion to reliably demonstrating more extensive disease.

4.2.1. Conventional CT

Extralaryngeal spread can be considered if the following features can be identified: substitution by tumor tissue on the outside of the membrane/cartilage, or loss of fat attenuation between the extralaryngeal structure (such as blood vessel or muscle) and laryngeal components. To detect extralaryngeal spread, it is important to thoroughly understand the complex anatomy in this area and the imaging features of commonly occurring extension patterns (Fig. 11). One of the most common routes of lesion spread from the larynx through areas of inherent weakness is via the thyrohyoid membrane (Fig. 12). The superior laryngeal neurovascular bundle enters the laryngeal component through a posterolateral defect in the thyrohyoid membrane; this defect is known to be the route by which tumors spread [48,49]. Another route of extralaryngeal spread, especially in the case of piriform sinus cancer, is via the inferior pharyngeal constrictor muscle [48,50] on the basis of its attachment to the lamina of the thyroid cartilage (Fig. 13). Sometimes, the tumor may show submucosal extension to the extralaryngeal soft tissue via the cricothyroid membrane (Fig. 14). Such extension into deep-seated tissue planes is difficult to evaluate by clinical inspection examination alone.

4.2.2. MR imaging

Diagnosis of extralaryngeal spread on the basis of MR imaging is based mainly on altered signal behavior of extralaryngeal soft tissue with different pulse sequences. Extralaryngeal spread is considered to be present when signals in the fat component of extralaryngeal soft tissue continuous with the primary tumor have an intensity similar to that of the tumor on T2WI, are hypointense on T1WI, and hyperintense on contrast-enhanced T1WI.

4.2.3. Dual-energy CT

Extralaryngeal spread can be identified on CT or MR imaging, but dual-energy CT may facilitate a clearer diagnosis. The IO images generated by using dual-energy CT reveal the area of tumor spread into soft tissue as red-colored enhancement, because IO images visualize areas of iodine distribution in soft tissue (Figs. 12B, 13B and 14C). The preliminarily reported sensitivity and specificity of WA plus IO images for extralaryngeal spread are 100% (14/14) and 100% (16/16), respectively [16]. Regardless of whether cartilage invasion is present, combined analysis of WA and IO images may also be useful for evaluating extralaryngeal spread of advanced laryngeal and hypopharyngeal cancer.

5. A diagnostic algorithm including dual-energy CT

All patients with symptoms that are suggestive of laryngeal or hypopharyngeal cancer should undergo a thorough assessment

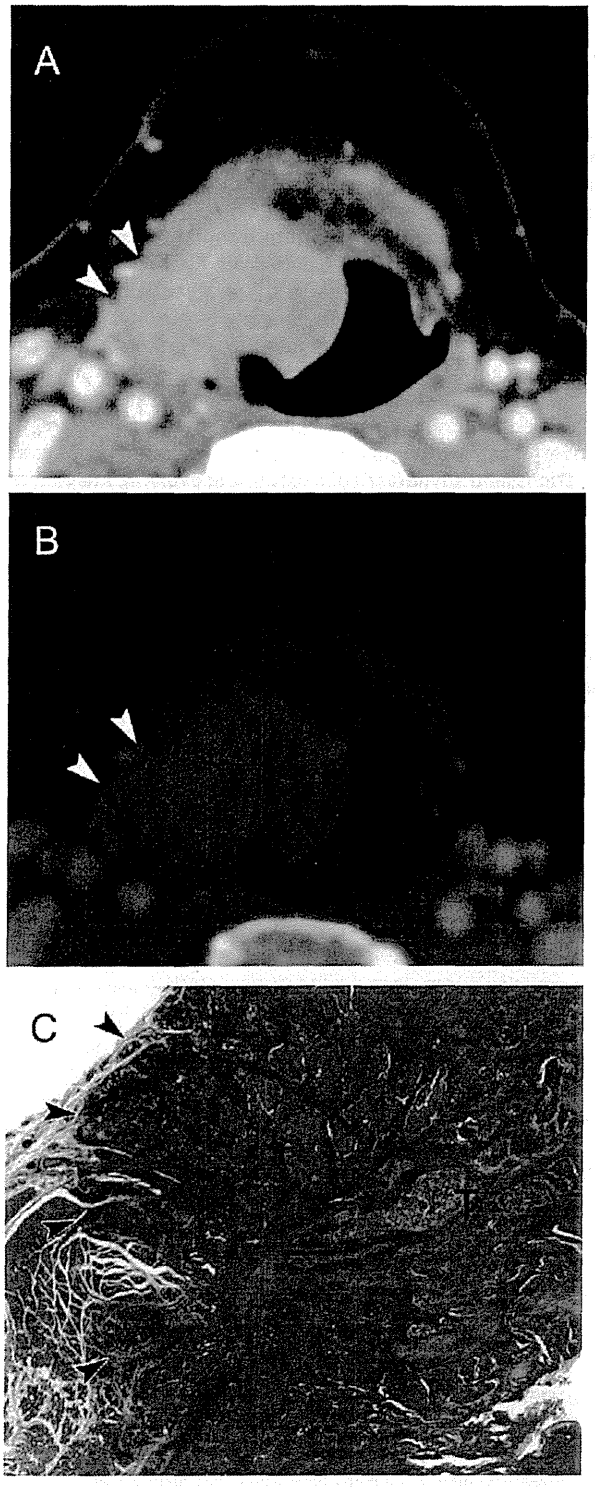

Fig. 12. Extralaryngeal spread via the thyrohyoid membrane on dual-energy CT in a 78-year-old man with supraglottic cancer. (A) WA image shows that the tumor has invaded the right aryepiglottic fold and preepiglottic space at the superior margin of the thyroid cartilage. The tumor extends through the thyrohyoid membrane into the extralaryngeal tissues (arrowheads). (B) The IO image reveals extralaryngeal tumor spread more clearly through the thyrohyoid membrane along the superior neurovascular bundle as a red-colored area (arrowheads). (C) Microscopic analysis confirmed the infiltration of the tumor cells into the extralaryngeal soft tissue and thyrohyoid muscle (*hematoxylin–eosin stain; original magnification, 5×*).

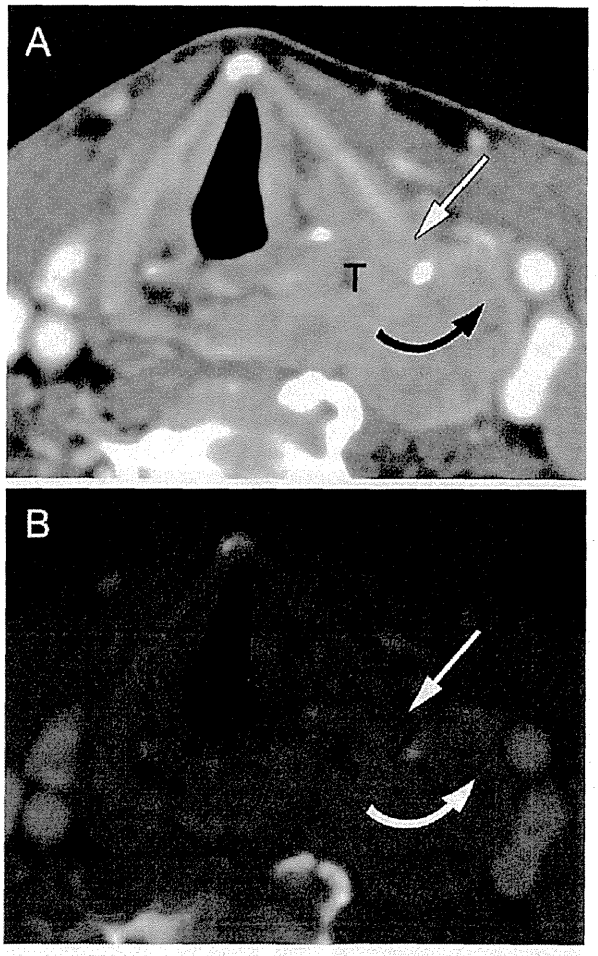

Fig. 13. Extralaryngeal spread via the inferior pharyngeal constrictor muscle on dual-energy CT in a 60-year-old man with hypopharyngeal cancer. WA image (A) and IO image (B) at the glottic level show a tumor mass (T) arising from the left piriform sinus, spreading into the lateral extralaryngeal soft tissue via the attachment of the inferior pharyngeal constrictor muscle (curved arrow). The tumor also wraps around the posterior border of the thyroid cartilage. On the WA image (A), the inner cortex of the left thyroid cartilage shows focal lysis (arrow). However, the IO image (B) shows no corresponding enhancement in the region indicated in the WA image (arrow). This case was evaluated as T4a disease without cartilage invasion and treated by chemoradiotherapy.

of their clinical history and a physical examination including nasopharyngoscopy, followed by multimodality imaging. We believe that dual-energy CT has the potential to become the primary diagnostic tool for laryngeal and hypopharyngeal cancer, although further investigation of dual-energy CT in comparison with MR will be necessary. Dual-energy CT may be very helpful for staging, including the definition of T stage, particularly when distinguishing T4 from lower-stage lesions, and for detection of regional lymph nodes (N staging) and distant metastasis (M staging). If evaluations conducted using dual-energy CT alone are insufficient, contrast-enhanced MR imaging is useful for excluding cartilage invasion, and for evaluation of very advanced local disease such as tumor invasion to the prevertebral fascia or carotid artery.

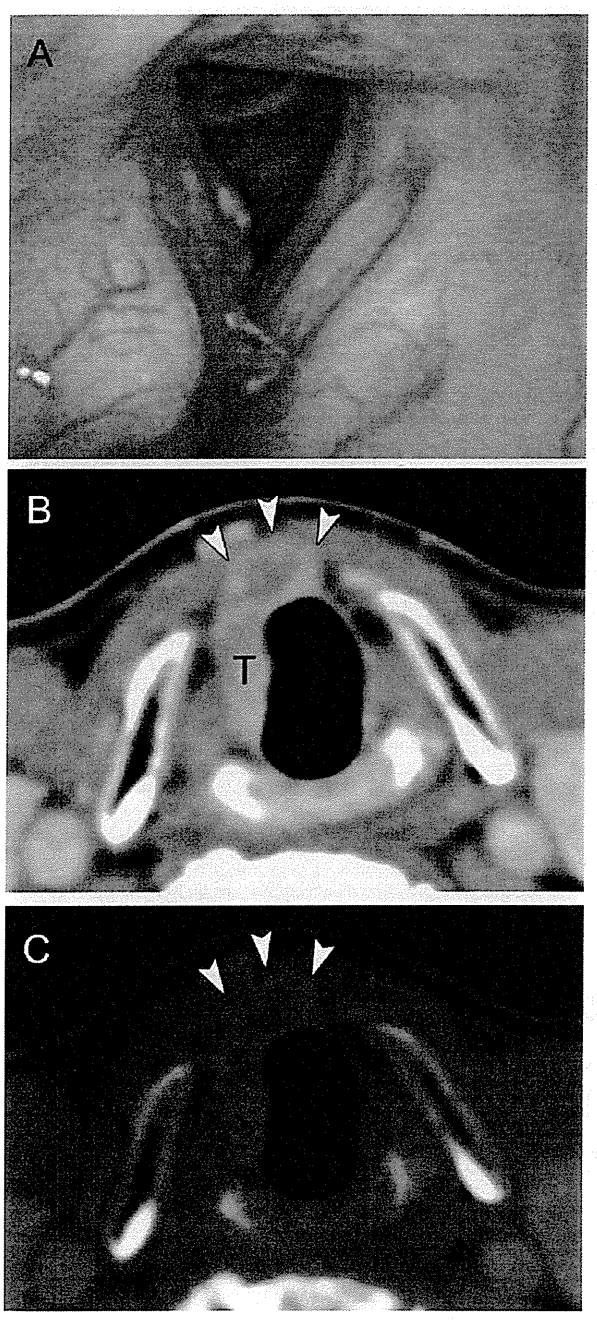

Fig. 14. Extralaryngeal spread via the cricothyroid membrane on dual-energy CT in a 72-year-old man with right glottic cancer. (A) Nasopharyngolaryngoscopy demonstrates the tumor mass (T) at the right glottis. It is diagnosed clinically as T3. WA image (B) and IO image (C) at the subglottic level show that the tumor has spread submucosally into the extralaryngeal soft tissue (arrowheads) via the cricothyroid membrane, and is therefore diagnosed as T4a.

6. Conclusion

Imaging plays a significant role in the staging of laryngeal and hypopharyngeal cancer, particularly when distinguishing the absence or presence of laryngeal cartilage invasion by the tumor and extralaryngeal spread. With conventional CT, although cartilage invasion can be diagnosed with acceptable accuracy by applying defined criteria for combinations of erosion, lysis and transmural extralaryngeal spread, iodine-enhanced tumors and non-ossified cartilage are sometimes difficult to distinguish. MR offers high contrast resolution for images without motion artifacts, although inflammatory changes in cartilage sometimes resemble cartilage invasion. With dual-energy CT, combined iodine-overlay images and weighted-average images can be used for evaluation of cartilage invasion, since iodine enhancement is evident in tumor tissue but not in cartilage. Extralaryngeal spread can be evaluated from CT, MR or dual-energy CT images and the three common routes of tumor spread into the extralaryngeal soft tissue must be considered. The ability to obtain weighted-average images and iodine-overlay images gives dual-energy CT potential advantages over conventional CT for evaluation of laryngeal and hypopharyngeal cancer. The benefit of the dual-energy technique lies in the impact of its high-quality images on treatment decision-making. Further advances in dual-energy CT may lead to its more widespread use for imaging of laryngeal and hypopharyngeal cancer. To define the most appropriate treatment strategies, it is important to thoroughly understand the potential applications, limitations, and advantages of existing and evolving imaging technologies, including dual-energy CT.

Conflict of interest

One of the authors (K.O.) is an employee of Siemens Japan. Authors who are not employees of Siemens Japan monitored and had control of inclusion of any data and information submitted for publication. No potential conflicts of interest were disclosed.

Acknowledgement

This work was supported in part by a National Cancer Center Research and Development Fund (23-A-35).

References

[1] Barnes L, Eveson JW, Riechart P, et al. 8edrs pathology and genetics of head and neck tumours. World Health Organization Classification of Tumours. Lyon: IARC; 2005. p. 107–62.
[2] Pfister DG, Laurie SA, Weinstein GS, et al. American Society of Clinical Oncology clinical practice guideline for the use of larynx-preservation strategies in the treatment of laryngeal cancer. J Clin Oncol 2006;24(22):3693–704.
[3] Hoffman HT, Porter K, Karnell LH, et al. Laryngeal cancer in the United States: changes in demographics, patterns of care, and survival. Laryngoscope 2006;116(9 Pt 2 Suppl 111):1–13.
[4] Forastiere AA, Goepfert H, Maor M, et al. Concurrent chemotherapy and radiotherapy for organ preservation in advanced laryngeal cancer. N Engl J Med 2003;349(22):2091–8.
[5] Knab BR, Salama JK, Solanki A, et al. Functional organ preservation with definitive chemoradiotherapy for T4 laryngeal squamous cell carcinoma. Ann Oncol 2008;19(9):1650–4.
[6] Worden FP, Moyer J, Lee JS, et al. Chemoselection as a strategy for organ preservation in patients with T4 laryngeal squamous cell carcinoma with cartilage invasion. Laryngoscope 2009;119(8):1510–7.
[7] Castelijns JA, Becker M, Hermans R. Impact of cartilage invasion on treatment and prognosis of laryngeal cancer. Eur Radiol 1996;6(2):156–69.
[8] Hermans R. Staging of laryngeal and hypopharyngeal cancer: value of imaging studies. Eur Radiol 2006;16(11):2386–400.
[9] Li B, Bobinski M, Gandour-Edwards R, Farwell DG, Chen AM. Overstaging of cartilage invasion by multidetector CT scan for laryngeal cancer and its potential effect on the use of organ preservation with chemoradiation. Br J Radiol 2011;84(997):64–9.
[10] Hartl DM, Landry G, Hans S, Marandas P, Brasnu DF. Organ preservation surgery for laryngeal squamous cell carcinoma: low incidence of thyroid cartilage invasion. Laryngoscope 2010;120(6):1173–6.
[11] Graser A, Johnson TR, Hecht EM, et al. Dual-energy CT in patients suspected of having renal masses: can virtual nonenhanced images replace true nonenhanced images? Radiology 2009;252(2):433–40.
[12] Gupta R, Phan CM, Leidecker C, et al. Evaluation of dual-energy CT for differentiating intracerebral hemorrhage from iodinated contrast material staining. Radiology 2010;257(1):205–11.
[13] Johnson TR, Krauss B, Sedlmair M, et al. Material differentiation by dual energy CT: initial experience. Eur Radiol 2007;17(6):1510–7.
[14] Kang MJ, Park CM, Lee CH, Goo JM, Lee HJ. Dual-energy CT: clinical applications in various pulmonary diseases. Radiographics 2010;30(3):685–98.

[15] Leschka S, Stolzmann P, Baumuller S, et al. Performance of dual-energy CT with tin filter technology for the discrimination of renal cysts and enhancing masses. Acad Radiol 2010;17(4):526–34.
[16] Kuno H, Onaya H, Iwata R, et al. Evaluation of cartilage invasion by laryngeal and hypopharyngeal squamous cell carcinoma with dual-energy CT. Radiology 2012;265(2):488–96.
[17] Sulfaro S, Barzan L, Querin F, et al. T staging of the laryngohypopharyngeal carcinoma. A 7-year multidisciplinary experience. Arch Otolaryngol Head Neck Surg 1989;115(5):613–20.
[18] Zbaren P, Becker M, Lang H. Pretherapeutic staging of laryngeal carcinoma. Clinical findings, computed tomography, and magnetic resonance imaging compared with histopathology. Cancer 1996;77(7):1263–73.
[19] Becker M, Burkhardt K, Dulguerov P, Allal A. Imaging of the larynx and hypopharynx. Eur J Radiol 2008;66(3):460–79.
[20] Edge SB BD, Compton CC, et al. (edrs) AJCC Cancer Staging Handbook (ed 7), New York, NY, Springer2010.
[21] Mendenhall WM, Parsons JT, Mancuso AA, Pameijer FJ, Stringer SP, Cassisi NJ. Definitive radiotherapy for T3 squamous cell carcinoma of the glottic larynx. J Clin Oncol 1997;15(6):2394–402.
[22] Mendenhall WM, Werning JW, Hinerman RW, Amdur RJ, Villaret DB. Management of T1–T2 glottic carcinomas. Cancer 2004;100(9):1786–92.
[23] Murakami R, Nishimura R, Baba Y, et al. Prognostic factors of glottic carcinomas treated with radiation therapy: value of the adjacent sign on radiological examinations in the sixth edition of the UICC TNM staging system. Int J Radiat Oncol Biol Phys 2005;61(2):471–5.
[24] Baum U, Greess H, Lell M, Nomayr A, Lenz M. Imaging of head and neck tumors - methods: CT, spiral-CT, multislice-spiral-CT. Eur J Radiol 2000;33(3): 153–60.
[25] Lell MM, Greess H, Hothorn T, Janka R, Bautz WA, Baum U. Multiplanar functional imaging of the larynx and hypopharynx with multislice spiral CT. Eur Radiol 2004;14(12):2198–205.
[26] Becker M, Zbaren P, Delavelle J, et al. Neoplastic invasion of the laryngeal cartilage: reassessment of criteria for diagnosis at CT. Radiology 1997;203(2):521–32.
[27] Brown CL, Hartman RP, Dzyubak OP, et al. Dual-energy CT iodine overlay technique for characterization of renal masses as cyst or solid: a phantom feasibility study. Eur Radiol 2009;19(5):1289–95.
[28] Karlo C, Lauber A, Gotti RP, et al. Dual-energy CT with tin filter technology for the discrimination of renal lesion proxies containing blood, protein, and contrast-agent. An experimental phantom study Eur Radiol 2011;21(2):385–92.
[29] Alvarez RE, Macovski A. Energy-selective reconstructions in X-ray computerized tomography. Phys Med Biol 1976;21(5):733–44.
[30] Hounsfield GN. Computerized transverse axial scanning (tomography). 1. Description of system. Br J Radiol 1973;46(552):1016–22.
[31] Kalender WA, Perman WH, Vetter JR, Klotz E. Evaluation of a prototype dual-energy computed tomographic apparatus.1. Phantom studies. Med Phys 1986;13(3):334–9.
[32] Kaza RK, Platt JF, Cohan RH, Caoili EM, Al-Hawary MM, Wasnik A. Dual-energy CT with single- and dual-source scanners: current applications in evaluating the genitourinary tract. Radiographics 2012;32(2):353–69.
[33] Krauss B, Schmidt B, Flohr T. Dual source CT. In: Johnson TRC, Fink C, Schönberg SO, Reiser MF, editors. Dual energy CT in clinical practice. 1st ed. Heidelberg, Dordrecht, London, New York: Springer; 2011. p. 11–20.
[34] Flohr TG, McCollough CH, Bruder H, et al. First performance evaluation of a dual-source CT (DSCT) system. Eur Radiol 2006;16(2):256–68.
[35] Tawfik AM, Kerl JM, Razek AA, et al. Image quality and radiation dose of dual-energy CT of the head and neck compared with a standard 120-kVp acquisition. AJNR Am J Neuroradiol 2011;32(11):1994–9.
[36] Paul J, Bauer RW, Maentele W, Vogl TJ. Image fusion in dual energy computed tomography for detection of various anatomic structures—effect on contrast enhancement, contrast-to-noise ratio, signal-to-noise ratio and image quality. Eur J Radiol 2011.
[37] Becker M. Neoplastic invasion of laryngeal cartilage: radiologic diagnosis and therapeutic implications. Eur J Radiol 2000;33(3):216–29.
[38] Becker M, Zbaren P, Laeng H, Stoupis C, Porcellini B, Vock P. Neoplastic invasion of the laryngeal cartilage: comparison of MR imaging and CT with histopathologic correlation. Radiology 1995;194(3):661–9.
[39] Beitler JJ, Muller S, Grist WJ, et al. Prognostic accuracy of computed tomography findings for patients with laryngeal cancer undergoing laryngectomy. J Clin Oncol 2010;28(14):2318–22.
[40] Nix PA, Salvage D. Neoplastic invasion of laryngeal cartilage: the significance of cartilage sclerosis on computed tomography images. Clin Otolaryngol Allied Sci 2004;29(4):372–5.
[41] Schmalfuss IM, Mancuso AA, Tart RP. Arytenoid cartilage sclerosis: normal variations and clinical significance. AJNR Am J Neuroradiol 1998;19(4):719–22.
[42] Munoz A, Ramos A, Ferrando J, et al. Laryngeal carcinoma: sclerotic appearance of the cricoid and arytenoid cartilage—CT-pathologic correlation. Radiology 1993;189(2):433–7.
[43] Gilbert K, Dalley RW, Maronian N, Anzai Y. Staging of laryngeal cancer using 64-channel multidetector row CT: comparison of standard neck CT with dedicated breath-maneuver laryngeal CT. Am J Neuroradiol 2010;31(2):251–6.
[44] Castelijns JA, Gerritsen GJ, Kaiser MC, et al. Invasion of laryngeal cartilage by cancer: comparison of CT and MR imaging. Radiology 1988;167(1):199–206.
[45] Becker M, Zbaren P, Casselman JW, Kohler R, Dulguerov P, Becker CD. Neoplastic invasion of laryngeal cartilage: reassessment of criteria for diagnosis at MR imaging. Radiology 2008;249(2):551–9.
[46] Hermans R, VanderGoten A, Baert AL. Image interpretation in CT of laryngeal carcinoma: a study on intra- and interobserver reproducibility. Eur Radiol 1997;7(7):1086–90.
[47] Hoorweg JJ, Kruijt RH, Heijboer RJJ, Eijkemans MJC, Kerrebijn JDF. Reliability of interpretation of CT examination of the larynx in patients with glottic laryngeal carcinoma. Otolaryngol Head Neck Surg 2006;135(1):129–34.
[48] Mancuso AA. Hypopharynx: malignant tumors. In: Mancuso AA, Hanafee WN, editors. Head and neck radiology. Philadelphia: Lippincott Williams & Wilkins; 2010. p. 2147–72.
[49] Mancuso AA. Larynx: malignant tumors. In: Mancuso AA, Hanafee WN, editors. Head and neck radiology. Philadelphia: Lippincott Williams & Wilkins; 2010. p. 1975–2022.
[50] Zbaren P, Egger C. Growth patterns of piriform sinus carcinomas. Laryngoscope 1997;107(4):511–8.

J Gastroenterol (2014) 49:932–940
DOI 10.1007/s00535-013-0853-7

The Japanese Society of Gastroenterology

ORIGINAL ARTICLE—LIVER, PANCREAS, AND BILIARY TRACT

Efficacy of sorafenib in patients with hepatocellular carcinoma refractory to transcatheter arterial chemoembolization

Masafumi Ikeda · Shuichi Mitsunaga · Satoshi Shimizu · Izumi Ohno · Hideaki Takahashi · Hiroyuki Okuyama · Akiko Kuwahara · Shunsuke Kondo · Chigusa Morizane · Hideki Ueno · Mitsuo Satake · Yasuaki Arai · Takuji Okusaka

Received: 5 March 2013 / Accepted: 9 June 2013 / Published online: 23 June 2013

Abstract
Background The efficacy of sorafenib for hepatocellular carcinoma (HCC) patients refractory to transcatheter arterial chemoembolization (TACE) has not yet been clarified. We investigated the efficacy of sorafenib in HCC patients who were refractory to TACE (sorafenib group) and retrospectively compared the results with those of patients treated with hepatic arterial infusion chemotherapy using cisplatin (cisplatin group).
Methods We evaluated the anti-tumor effect, the time to progression, and the overall survival in 48 patients in the sorafenib group and 66 patients in the cisplatin group.
Results The disease control rate to sorafenib was 60.4 %, the median time to progression was 3.9 months, and the median survival time was 16.4 months in patients who were refractory to TACE. When compared with the cisplatin group, significant differences in the patient characteristics were not observed between the two groups with the exception of patient age; however, the disease control rate (cisplatin group 28.8 %, $P = 0.001$), time to progression (cisplatin group: median 2.0 months, hazard ratio 0.44, $P < 0.01$), and overall survival (cisplatin group: median 8.6 months, hazard ratio 0.57, $P < 0.001$) were significantly superior in the sorafenib group. The multivariate analysis also showed the sorafenib treatment to be the most significant factor contributing to prolongation of time to progression and overall survival.
Conclusions Sorafenib showed favorable treatment results in patients refractory to TACE. When compared with hepatic arterial infusion chemotherapy using cisplatin, sorafenib demonstrated a significantly higher disease control rate, a longer time to progression and increased overall survival.

Keywords Hepatocellular carcinoma · Sorafenib · Cisplatin · Chemotherapy · Hepatic arterial infusion chemotherapy

Introduction

Hepatocellular carcinoma (HCC) is one of the most common malignancies worldwide. HCC is highly prevalent in African and Asian countries, and its incidence has recently been increasing in western countries [1, 2]. For patients with unresectable HCC who are not candidates for curative treatments, such as resection, transplantation, or local ablation, transcatheter arterial chemoembolization (TACE) is the main therapeutic option [1, 2]. A clear survival benefit for patients with unresectable HCC who are treated with TACE has been shown in several randomized controlled trials and a meta-analysis [3, 4]. Chemotherapy has been recognized as a palliative treatment option for patients with highly advanced HCC in whom TACE is not indicated.

Sorafenib is a multikinase inhibitor of Raf kinase, which is involved in cancer cell proliferation, as well as vascular

M. Ikeda (✉) · S. Mitsunaga · S. Shimizu · I. Ohno · H. Takahashi · H. Okuyama · A. Kuwahara
Division of Hepatobiliary and Pancreatic Oncology, National Cancer Center Hospital East, 6-5-1 Kashiwanoha, Kashiwa, Chiba 277-8577, Japan
e-mail: masikeda@east.ncc.go.jp

S. Kondo · C. Morizane · H. Ueno · T. Okusaka
Hepatobiliary and Pancreatic Oncology Division, National Cancer Center Hospital, Tokyo, Japan

M. Satake
Division of Diagnostic Radiology, National Cancer Center Hospital East, Kashiwa, Japan

Y. Arai
Department of Diagnostic Radiology, National Cancer Center Hospital, Tokyo, Japan

endothelial growth factor receptor-2/-3 (VEGFR-2/-3) and platelet-derived growth factor receptor beta (PDGFR-β), which is involved in peritumor neovascularization [5, 6]. In two pivotal international phase 3 trials of sorafenib vs. placebo, the so-called SHARP trial [7] and the Asia-Pacific trial [8], sorafenib demonstrated a prolonged overall survival and time-to-progression, compared with a placebo, in patients with advanced hepatocellular carcinoma (HCC). Therefore, sorafenib has been acknowledged as a standard therapy for advanced HCC.

In the therapeutic strategy of the Barcelona Clinic Liver Cancer Study Group [5], sorafenib was indicated for patients with extrahepatic metastasis and/or vascular invasion of Stage C disease (advanced stage), patients with a performance status (PS) of 1–2, and those with Stage B (intermediate stage) multifocal HCC refractory to TACE. In the 2010 updated version of the consensus-based clinical practice guidelines for the management of HCC proposed by the Japan Society of Hepatology [9, 10], patients with extrahepatic metastasis, with macrovascular invasion, and who were refractory to TACE are listed in the algorithm for treatment with sorafenib. The main indications for sorafenib are, therefore, considered to be patients who are refractory to TACE, those who have vascular invasion, or those who have extrahepatic metastasis. Subgroup analyses of the SHARP trial [7] and the Asia-Pacific trial [8] showed the treatment efficacies in patients with vascular invasion and extrahepatic metastasis. However, those in patients who are refractory to TACE have not been reported so far, although the outcome of patients with prior TACE has been reported [11, 12].

Before the introduction of sorafenib, hepatic arterial infusion chemotherapy was mainly performed in Japan for patients with advanced HCC [13–21], including those refractory to TACE [13, 14]. However, no consensus on a standard therapy has been achieved because large-scale prospective studies and randomized controlled studies have not been conducted and the survival benefit has not been clarified [10]. In this study, we clarified the efficacy of sorafenib in patients who were refractory to TACE (sorafenib group) and retrospectively compared the anti-tumor effect, time to progression, and overall survival between the sorafenib group and patients who were refractory to TACE and who were treated with hepatic arterial infusion chemotherapy using cisplatin (cisplatin group).

Patients and methods

Patients

Forty-eight consecutive chemotherapy-naive patients who were refractory to TACE without extrahepatic metastasis were extracted from 205 patients treated with sorafenib at the National Cancer Center Hospital East (East Hospital) between April 2009 and December 2011. Sixty-six of the 84 chemo-naive patients who were refractory to TACE and were treated with hepatic arterial infusion chemotherapy using cisplatin at the National Cancer Center Hospital and the East Hospital between July 2004 and September 2008, the period before the approval of sorafenib in Japan, were enrolled in the cisplatin group after excluding 18 patients with extrahepatic metastasis or the moderate retention of ascites. In this series, the total number of TACE sessions was 478, while the median number of TACE sessions was 4 (range 1–16). In previous TACE sessions, an emulsion containing an anticancer agent and lipiodol followed by gelatin sponge particles were used. In the present series, epirubicin was used for 394 sessions, adriamycin was used for 29 sessions, and mitomycin C was used for 12 sessions; the anticancer agent was unknown for 43 sessions. Patients who were refractory to TACE were defined as those showing progression or a tumor shrinkage rate of <25 % of the hypervascular lesions as visualized using dynamic computed tomography (CT) and/or magnetic resonance imaging (MRI) after 1–3 months of TACE [13]. The TACE-refractory status of individual patients was discussed at a weekly tumor board conference. HCC was diagnosed based on the presence of histopathological findings or imaging findings that were characteristic of HCC together with an increase in the serum α-fetoprotein level. The diameter of the tumor and the presence/absence of extrahepatic metastasis were confirmed using dynamic CT/MRI, ultrasound, or chest X-ray/CT prior to treatment. In our hospital, sorafenib is indicated for the treatment of patients with highly advanced HCC with a Child–Pugh score of either A or B. Informed consent for each treatment was obtained from all the patients before the initiation of treatment. This clinical study was conducted with the approval of the Ethics Committee of the National Cancer Center and was conducted in accordance with the ethical principals stated in the Japanese ethics guideline for epidemiological research.

Treatments

An oral dose of sorafenib at 400 mg was administered twice daily, after breakfast and dinner (800 mg/day). Treatment was continued as long as tolerability was observed without obvious disease progression. The dose was reduced or withdrawn and treatment was continued depending on the severity of adverse events. A dose increase up to 800 mg/day was permitted when the dose increase was judged possible in patients in whom the dose had been reduced.

For hepatic arterial infusion chemotherapy using cisplatin, intra-arterial cisplatin at a dose of 65 mg/m^2 was

administered over 20–40 min via a catheter inserted into the feeding arteries of the tumors. Treatment was repeated every 4–6 weeks for up to 6 courses until disease progression or unacceptable toxicities occurred. An infusion of 3,000 mL or more was administered on the day of treatment, and an infusion of 1,000 mL or more was continued for 3 days after administration to reduce renal toxicity caused by cisplatin; a diuretic (mannitol, furosemide, etc.) was administered as necessary to ensure an adequate urine volume.

Assessment and statistical analyses

Dynamic CT or MRI was used to confirm the anti-tumor effect every 1–2 months. The anti-tumor effect was evaluated using the Response Evaluation Criteria in Solid Tumors, version 1.0 (RECIST) [22], to judge the best overall response. The time to progression was defined as the period from the date of the start of treatment until the date of the confirmation of tumor progression by radiological evaluation or the day on which obvious tumor progression was judged to have occurred based on the clinical symptoms. Overall survival was defined as the period from the day of the start of treatment until the date of death or the final date of confirmed survival. A χ^2 test or Wilcoxon test was used to compare the patient characteristics and the anti-tumor effect between the sorafenib and the hepatic arterial infusion chemotherapy using cisplatin groups, and the Kaplan–Meier method was used to calculate the time to progression and the overall survival; the log-rank test was used to analyze differences between the groups. In a multivariate analysis, a Cox regression was used to analyze factors with $P < 0.10$ using a univariate analysis. $P < 0.05$ was judged to be statistically significant. JMP version 9.0 (SAS Institute Inc.) was used for the above statistical analyses.

Results

Patient characteristics

Table 1 shows the patient characteristics before each treatment. Age was significantly higher in the sorafenib group, although the medians were very similar (sorafenib group 71 years, cisplatin group 69 years). Although the Eastern Cooperative Oncology Group PS, the maximum tumor diameter, total bilirubin, AST, and ALT tended to be slightly worse in the cisplatin group, significant differences were not observed in the other parameters between the two groups. The median number of treatments in the cisplatin group was 2 (range 1–6 times). As a subsequent treatment, other systemic chemotherapy was performed in 14 patients, hepatic arterial infusion chemotherapy using cisplatin was performed in 7 patients, TACE was performed in 4 patients, and hepatic arterial infusion chemotherapy using 5-FU + interferon and radiotherapy was performed in one patient each in the sorafenib group; meanwhile, TACE was performed in 15 patients, hepatic arterial infusion chemotherapy using epirubicin was performed in 4 patients, other systemic chemotherapy was performed in 4 patients, hepatic arterial infusion chemotherapy using 5-FU + interferon was performed in 2 patients, and radiotherapy was performed in one patient in the cisplatin group. The median observation period was 9.4 months (range 2.1–31.6 months) in the sorafenib group and 7.5 months (range 0.8–43.1 months) in the cisplatin group; this difference was not statistically significant ($P = 0.44$).

Efficacy

The best overall response in the sorafenib group was evaluated as a complete response (CR) in one patient, a partial response (PR) in 2 patients, stable disease (SD) in 26 patients, progressive disease (PD) in 16 patients, and not evaluable (NE) in 3 patients. The response rate (CR + PR) was 6.3 % [95 % confidence interval (CI) 1.3–17.2 %], and the disease control rate (CD + PR + SD) was 60.4 % (95 % CI 45.3–74.2 %). The median time to progression and the progression-free rate at 6- and 12-months were 3.9 months, 32.6 %, and 12.1 %, respectively, while the median overall survival and the survival rate at 6-, 12-, and 24-months was 16.4 months, 88.9 %, 55.3 %, and 32.5 %, respectively, in the sorafenib group.

The best overall response in the cisplatin group was evaluated as a CR in 1 patient, PR in 0 patients, SD in 18 patients, PD in 39 patients, and NE in 8 patients. The response rate was 1.5 % (95 % CI 0.04–8.2 %), and a significant difference in the response rate, compared with the sorafenib group, was not observed ($P = 0.40$). The disease control rate was 28.8 % (95 % CI 18.3–41.3 %), which was significantly higher in the sorafenib group ($P = 0.001$). The median time to progression and the progression-free rate at 6- and 12-months in the cisplatin group was 2.0 months, 15.9 %, and 4.8 %, respectively, showing a significantly superior result in the sorafenib group (hazard ratio 0.44, $P < 0.01$) (Fig. 1). At the time of analysis, 21 patients had died because of tumor progression, and 1 patient had died because of hepatic failure in the sorafenib group. Additionally, 60 patients had died because of tumor progression, and 4 patients had died because of hepatic failure in the cisplatin group. The median survival time and the survival rate at 6-, 12-, and 24-months in the cisplatin group were 8.6 months, 62.0 %, 35.2 %, and 11.3 %, respectively, showing a significantly superior result in the sorafenib group (hazard ratio: 0.57,

Table 1 Patient characteristics

	Sorafenib		Cisplatin		*P* value
	n	(%)	*n*	(%)	
All patients	48	–	66	–	
Age (years)					
Median [range]	71	[53–83]	69	[40–82]	0.04
Sex					
Male	43	(90)	52	(79)	
Female	5	(10)	14	(21)	1.00
Performance status					
0	43	(90)	49	(74)	
1	5	(10)	17	(26)	0.07
HCVAb (positive)	32	(67)	45	(68)	1.00
HBsAg (positive)	7	(15)	8	(12)	0.92
Prior resection (present)	12	(25)	27	(41)	0.11
Prior ablation (present)	19	(40)	29	(44)	1.00
No. of prior TACE sessions					
Median [range]	4	[1–9]	4	[1–17]	0.86
Maximum tumor diameter (mm)					
Median [range]	30.5	[10–150]	40	[12–110]	0.07
Number of tumors					
1–3	8	(17)	13	(20)	0.32
≥4	40	(83)	53	(80)	0.64
Portal vein invasion (present)	9	(19)	16	(24)	0.64
Hepatic vein invasion (present)	3	(6)	4	(6)	0.99
Stage[a]					
II or III	38	(79)	49	(74)	
IVa	10	(21)	17	(26)	0.70
Ascites (present)	9	(19)	17	(26)	0.51
Child–Pugh class					
A	32	(67)	36	(55)	
B	16	(33)	30	(45)	0.27
Total bilirubin (mg/dL)					
Median [range]	0.9	[0.3–2.1]	1.1	[0.2–3.0]	0.02
Albumin (g/dL)					
Median [range]	3.5	[2.3–4.8]	3.3	[2.4–4.5]	0.21
AST (U/L)					
Median [range]	54	[20–165]	88	[35–287]	0.04
ALT (U/L)					
Median [range]	43	[10–139]	62	[22–187]	0.05
Prothrombin time (%)					
Median [range]	78	[40–107]	73	[48–104]	0.39
α-Fetoprotein (ng/mL)					
Median [range]	70.3	[1.3–218876]	324.3	[1.7–210200]	0.59
PIVKAII (mAU/mL)					
Median [range]	505.5	[11–291330]	438	[11–96390]	0.65
Subsequent treatments (present)	27	(56)	26	(39)	0.11

HCVAb hepatitis C viral antibody, *HBsAg* hepatitis B surface antigen, *TACE* transcatheter arterial chemoembolization, *AST* aspartate aminotransferase, *ALT* alanine aminotransferase, *PIVKAII* protein induced by vitamin K absence or antagonists-II

[a] Japanese classification of primary liver cancer

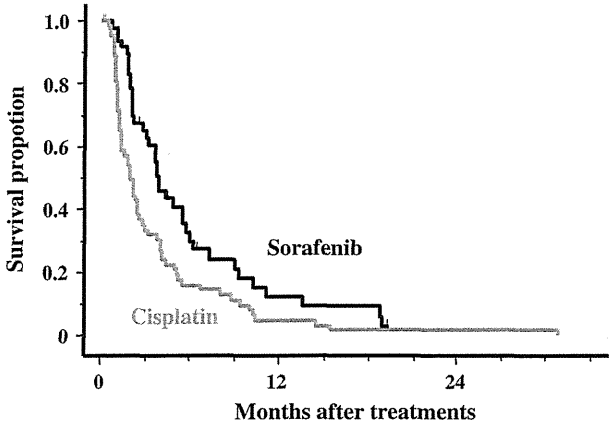

Fig. 1 Comparison of time to progression between sorafenib and hepatic arterial infusion chemotherapy using cisplatin in patients who were refractory to transcatheter arterial chemoembolization (TACE)

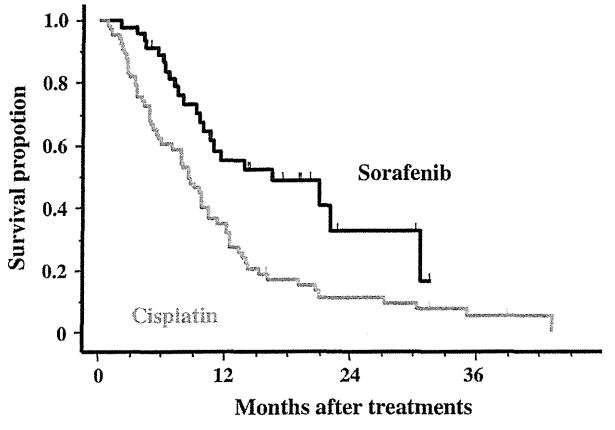

Fig. 2 Comparison of overall survival between sorafenib and hepatic arterial infusion chemotherapy using cisplatin in patients who were refractory to TACE

$P < 0.001$) (Fig. 2). The same analysis was performed for patients limited to Child–Pugh A, since sorafenib is widely recommended for the treatment of patients with Child–Pugh A. The results were similar, although the disease control rate and the time to progression were not statistically significant (data not shown).

Toxicity

Serious adverse events (SAE) occurred in two patients (1 patient, grade 4 hepatic encephalopathy; 1 patient, grade 3 erythema multiforme) in the sorafenib group, but none of the patients in the cisplatin group experienced an SAE. Thirty-eight patients (79 %) required a sorafenib dose reduction because of adverse events, such as liver dysfunction, hand-foot syndrome, or rashes, and treatment was discontinued in 7 patients (14 %) because of adverse events, such as liver dysfunction, hepatic encephalopathy, or erythema multiforme. On the other hand, none of the patients required a cisplatin dose reduction, and treatment was discontinued in 6 patients (9.1 %) because of adverse events, such as liver dysfunction, fatigue, or nausea/anorexia.

Predictive factors of time to progression and overall survival

Univariate analyses were performed to identify the factors that contributed to the prolongation of time to progression in patients who were refractory to TACE (Table 2). The univariate analyses showed that the significant factors that contributed to the prolongation of the time to progression ($P < 0.10$) were an age >65 years, a PS of 0, a maximum tumor diameter ≤3.0 cm, the absence of hepatic vein invasion, the absence of ascites, a bilirubin level ≤1.2 mg/dL, an α-fetoprotein level <1,000 ng/mL, and sorafenib treatment. A multivariate analysis was performed for the factors that showed a significant tendency ($P < 0.10$) in the univariate analysis, and the absence of hepatic vein invasion and sorafenib treatment were significant independent factors that contributed to the prolongation of the time to progression (Table 3). Univariate analyses were performed to identify the factors that contributed to survival prolongation in patients who were refractory to TACE (Table 2). The univariate analyses showed that the significant factors that contributed to the prolongation of survival ($P < 0.10$) were an age >65 years, a PS of 0, a maximum tumor diameter of ≤3.0 cm, 3 or fewer tumors, the absence of hepatic vein invasion, Child–Pugh class A, the absence of ascites, an albumin level >3.5 g/dL, a bilirubin level ≤1.2 mg/dL, an AST level <100 U/L, an α-fetoprotein level <1,000 ng/mL, a protein induced by vitamin K absence or antagonist-II (PIVKA-II) level <1,000 mAU/mL, and sorafenib treatment. A multivariate analysis was performed for the factors showing a significant tendency at $P < 0.10$, and the significant independent favorable prognosis factors were a PS of 0, 3 or fewer tumors, Child–Pugh A, an α-fetoprotein level <1,000 ng/mL, a PIVKA-II level <1,000 mAU/mL, and treatment with sorafenib (Table 3). Treatment with sorafenib had the smallest hazard ratio among these prognostic factors.

Discussion

Patients with vascular invasion, extrahepatic metastasis, and who are refractory to TACE are good candidates for sorafenib [5, 9, 10]. However, the efficacy of sorafenib in patients who are refractory to TACE has not been previously reported, although the outcome of patients with prior

Table 2 Univariate analysis of time to progression and overall survival time in patients refractory to transcatheter arterial chemoembolization treated with sorafenib or intra-arterial cisplatin

	n	Time to progression			Overall survival		
		Median (months)	Hazard ratio	*P* value	Median (months)	Hazard ratio	*P* value
Sex							
Female	19	2.9	1.01 (0.60–1.68)	0.98	10.5	0.92 (0.51–1.68)	0.79
Male	95	2.6			9.8		
Age (years)							
≤65	33	2.0	1.41 (0.92–2.14)	0.11	8.0	1.65 (1.03–2.66)	0.03
>65	81	3.0			11.4		
Performance status							
0	92	3.2	0.58 (0.35–0.95)	0.03	11.4	0.38 (0.22–0.66)	<0.001
1–2	22	1.6			4.8		
HCVAb							
Negative	37	2.8	0.82 (0.53–1.25)	0.35	9.9	0.72 (0.45–1.18)	0.19
Positive	77	2.5			9.8		
HBsAg							
Negative	99	3.0	0.86 (0.50–1.50)	0.60	9.9	1.09 (0.54–2.17)	0.82
Positive	15	2.1			9.8		
Maximum tumor diameter (cm)							
≤3.0	39	4.0	0.65 (0.43–0.99)	0.04	12.3	0.56 (0.34–0.83)	0.02
>3.0	75	2.2			8.7		
No. of tumors							
≤3	21	4.4	0.78 (0.48–1.29)	0.33	13.8	0.68 (0.39–1.19)	0.06
>3	93	2.4			8.0		
Portal vein invasion							
Present	25	3.2	0.89 (0.55–1.43)	0.62	5.4	1.34 (0.79–2.27)	0.23
Absent	89	2.6			8.7		
Hepatic vein invasion							
Present	7	2.5	2.12 (0.97–4.66)	0.05	4.8	2.17 (0.94–5.03)	0.13
Absent	107	2.8			9.2		
Stage[a]							
II or III	87	2.8	0.94 (0.59–1.48)	0.77	11.6	0.64 (0.39–1.07)	0.08
IV	27	2.5			6.2		
Child–Pugh class							
A	68	3.2	0.84 (0.56–1.26)	0.39	9.5	0.65 (0.41–1.01)	0.08
B	46	2.2			7.8		
Ascites							
Present	26	2.2	1.56 (0.98–2.47)	0.06	5.6	2.15 (1.32–3.53)	0.01
Absent	88	2.9			9.2		
Albumin (g/dL)							
≤3.5	76	2.4	1.17 (0.78–1.77)	0.44	7.8	1.90 (1.16–3.11)	0.02
>3.5	38	3.8			10.6		
Total bilirubin (mg/dL)							
≤1.2	81	3.2	0.66 (0.42–1.02)	0.06	11.6	0.42 (0.26–0.66)	<0.001
>1.2	33	1.6			4.8		
Prothrombin time (%)							
<70	42	2.9	0.95 (0.63–1.42)	0.79	10.5	0.93 (0.59–1.47)	0.77
≥70	72	2.5			9.9		

Table 2 continued

	n	Time to progression			Overall survival		
		Median (months)	Hazard ratio	*P* value	Median (months)	Hazard ratio	*P* value
AST (U/L)							
<100	82	3.0	0.86 (0.55–1.35)	0.50	12.3	0.44 (0.27–0.70)	<0.001
≥100	32	2.2			5.5		
ALT (U/L)							
<100	97	2.6	0.90 (0.52–1.56)	0.70	9.9	0.85 (0.44–1.57)	0.59
≥100	17	2.5			8.5		
α-Fetoprotein (ng/mL)							
<1,000	71	3.8	0.60 (0.40–0.91)	0.01	12.2	0.61 (0.39–0.96)	0.03
≥1,000	43	2.1			7.1		
PIVKA-II (mAU/mL)							
<1,000	67	3.1	0.78 (0.52–1.16)	0.22	10.6	0.62 (0.40–0.96)	0.03
≥1,000	45	2.1			9.5		
Treatments							
Sorafenib	48	3.9	0.57 (0.38–0.86)	0.01	16.4	0.44 (0.27–0.72)	<0.001
Cisplatin	66	2.0			8.6		

HCVAb hepatitis C viral antibody, *HBsAg* hepatitis B surface antigen, *AST* aspartate aminotransferase, *ALT* alanine aminotransferase, *PIVKAII* protein induced by vitamin K absence or antagonists-II

[a] Japanese classification of primary liver cancer

Table 3 Multivariate analysis of overall survival and time to progression in patients refractory to TACE

	Hazard ratio	*P* value
Time to progression		
Hepatic vein invasion: present	0.41 (0.19–0.91)	0.03
Treatment: sorafenib	0.55 (0.37–0.83)	0.004
Overall survival		
Performance status: 0	0.46 (0.27–0.81)	0.006
No. of tumors: ≤3	0.51 (0.29–0.91)	0.02
Child–Pugh class: A	0.44 (0.27–0.71)	0.001
α-Fetoprotein: <1,000 ng/mL	0.52 (0.22–0.84)	0.008
PIVKA-II: <1,000 mAU/mL	0.47 (0.29–0.76)	0.002
Treatment: sorafenib	0.42 (0.25–0.77)	0.001

TACE has been reported [11, 12]. We retrospectively evaluated the efficacy of sorafenib in patients who were refractory to TACE. The following data were obtained: the response rate (CR + PR) was 6.3 %, the disease control rate (CD + PR + SD) was 60.4 %, and the median time to progression was 3.9 months; these results were comparable to those obtained for sorafenib to date [7, 8]. The median survival time of 16.4 months was regarded as favorable. The patients who were refractory to TACE have a lower frequency of vascular invasion, which is a significant predictor of a poor prognosis in patients with advanced HCC. In addition, most of the TACE refractory patients had an intermediate BCLC stage. The TACE refractory patients in this study (proportion of advanced stage 33 %) had a better BCLC stage than the patients in previous trials (proportion of advanced stage SHARP, 82 %; Asia-Pacific trial, 95.3 %). Favorable tendencies, therefore, might be shown for the overall survival of a subgroup of patients who are refractory to TACE among advanced HCC patients in whom sorafenib treatment is indicated.

A definition of "refractory to TACE" has not yet been established. In this study, the definition of "refractory to TACE" was regarded as progression or a tumor shrinkage rate of <25 % in hypervascular lesions as visualized using dynamic CT and/or MRI after 1–3 months of TACE. According to the consensus-based clinical practice guidelines proposed by the Japan Society of Hepatology 2010 [5], however, "refractory to TACE" is defined as two or over consecutive incomplete necrotic reactions or the appearance of a new lesion, vascular invasion, or extrahepatic metastases. Although a consensus has not been reached among clinicians, this is a critical issue when considering a conversion from TACE to sorafenib treatment in patients with unresectable HCC.

In the present study, sorafenib was compared with hepatic arterial infusion chemotherapy using cisplatin, which was used before the introduction of sorafenib. A consensus on a standard therapy has not been attained for hepatic arterial infusion chemotherapy, since its survival benefit has not been elucidated [10]. However, this regimen is still frequently used in Japan, because favorable antitumor effects and long-term survivals have been seen in a

few patients [15–21]. Nonetheless, hepatic arterial infusion chemotherapy has not been reported to have favorable results in patients who are refractory to TACE [13, 14]. Regarding hepatic arterial infusion chemotherapy using cisplatin in patients who were refractory to TACE ($n = 84$), the response rate at out-patient hospitals was 3.6 %, the median time to progression was 1.7 months, and the median overall survival period was 7.1 months [13], while the results of a phase II study of hepatic arterial infusion chemotherapy using cisplatin in patients with unresectable HCC ($n = 80$) were favorable, with a response rate of 33.8 % and a 1-year survival rate of 67.5 % [15]. One possible reason for the difference between these studies might be differences in the characteristics of the study populations. Most patients in the phase II trial of cisplatin were TACE-naïve, whereas only patients with TACE-refractory disease were included in the present study. Thus, hepatic arterial infusion chemotherapy may not be expected to show favorable therapeutic results when the patients are limited to those refractory to TACE, although the reason remains unknown. Therefore, the results were compared with those for patients who were refractory to TACE and were treated with sorafenib. Although the patient age was significantly higher in the sorafenib group and the PS and tumor size was slightly worse in the cisplatin group, no other significant differences in the patient characteristics were observed between the two groups. The response rate was comparable, but the sorafenib group showed significantly higher results for the disease control rate, time to progression, and overall survival. We also performed a multivariate analysis to examine the factors that contributed to the time to progression and overall survival in patients who were refractory to TACE, and treatment with sorafenib was one of the significant factors. These results suggest that sorafenib, rather than hepatic arterial infusion chemotherapy using cisplatin, might be the treatment of first choice in patients who are refractory to TACE. This outcome might not have much impact in overseas settings, where hepatic arterial infusion chemotherapy is less popular, but it is quite disappointing in Japan, since hepatic arterial infusion chemotherapy using cisplatin was expected to show a therapeutic effect comparable to that of sorafenib.

The present study has some limitations. First, the results for sorafenib treatment in patients who were refractory to TACE were obtained as part of a single-site, retrospective study. A prospective study enrolling only patients who are refractory to TACE should be performed in the future to verify the efficacy of sorafenib in patients who are refractory to TACE. Second, the periods of treatment differed between the sorafenib group and the cisplatin group. Third, the influence of subsequent treatment on the overall survival cannot be denied. Hepatic arterial infusion chemotherapy using cisplatin was administered as a subsequent treatment in 7 patients in the sorafenib group, whereas patients in the cisplatin group were not treated with sorafenib. Still, the anti-tumor effect of hepatic arterial infusion chemotherapy using cisplatin following sorafenib was PD in all the patients, and the impact would have been negligible. Finally, considering the possible selection bias in therapeutic policy after the introduction of sorafenib, we selected patients with different periods of treatment, but the results might also have been affected by the difference in periods. Also, no significant differences in the patient characteristics, except for age, total bilirubin, and AST, were seen between the sorafenib and the hepatic arterial infusion chemotherapy using cisplatin group, but subtle differences in the patient characteristics might have affected the favorable results for sorafenib, since this study was a retrospective comparison.

In conclusion, sorafenib showed a favorable efficacy in patients who were refractory to TACE, resulting in a significantly higher disease control rate, longer time to progression, and longer overall survival compared with hepatic arterial infusion chemotherapy using cisplatin. Thus, sorafenib, rather than hepatic arterial infusion chemotherapy, should be considered as the first-line therapy for patients who are refractory to TACE in the future.

Acknowledgments This work was supported in part by Grants-in-Aid for Cancer Research and for the Third-Term Comprehensive 10-Year Strategy for Cancer Control from the Ministry of Health, Labour, and Welfare of Japan.

Conflict of interest The authors declare that they have no conflict of interest.

References

1. Kudo M, Izumi N, Kokudo N, Matsui O, Sakamoto M, Nakashima O, et al. Management of hepatocellular carcinoma in Japan: consensus-based clinical practice guidelines proposed by the Japan Society of Hepatology (JSH) 2010 updated version. Dig Dis. 2011;29:339–64.
2. Bruix J, Sherman M, Practice Guidelines Committee, American Association for the Study of Liver Diseases. Management of hepatocellular carcinoma. Hepatology. 2005;42:1208–36.
3. Cammà C, Schepis F, Orlando A, Albanese M, Shahied L, Trevisani F, et al. Transarterial chemoembolization for unresectable hepatocellular carcinoma: meta-analysis of randomized controlled trials. Radiology. 2002;224:47–54.
4. Llovet JM, Bruix J. Systematic review of randomized trials for unresectable hepatocellular carcinoma: chemoembolization improves survival. Hepatology. 2003;37:429–42.
5. Llovet JM, Bruix J. Molecular targeted therapies in hepatocellular carcinoma. Hepatology. 2008;48:1312–27.
6. Zhu AX. Development of sorafenib and other molecularly targeted agents in hepatocellular carcinoma. Cancer. 2008;112:250–9.
7. Llovet JM, Ricci S, Mazzaferro V, Hilgard P, Gane E, Blanc JF, et al. Sorafenib in advanced hepatocellular carcinoma. N Engl J Med. 2008;359:378–90.

8. Cheng AL, Kang YK, Chen Z, Tsao CJ, Qin S, Kim JS, et al. Efficacy and safety of sorafenib in patients in the Asia-Pacific region with advanced hepatocellular carcinoma: a phase III randomised, double-blind, placebo-controlled trial. Lancet Oncol. 2009;10:25–34.
9. Kudo M, Izumi N, Kokudo N, Matsui O, Sakamoto M, Nakashima O, et al. Management of hepatocellular carcinoma in Japan: consensus-based clinical practice guidelines proposed by the Japan Society of Hepatology (JSH) 2010 updated version. Dig Dis. 2011;29:339–64.
10. Yamashita T, Kaneko S. Treatment strategies for hepatocellular carcinoma in Japan. Hepatol Res. 2013;43:44–50.
11. Bruix J, Raoul JL, Sherman M, Mazzaferro V, Bolondi L, Craxi A, et al. Efficacy and safety of sorafenib in patients with advanced hepatocellular carcinoma: subanalyses of a phase III trial. J Hepatol. 2012;57:821–90.
12. Cheng AL, Guan Z, Chen Z, Tsao CJ, Qin S, Kim JS, et al. Efficacy and safety of sorafenib in patients with advanced hepatocellular carcinoma according to baseline status: subset analyses of the phase III Sorafenib Asia-Pacific trial. Eur J Cancer. 2012;48:1452–65.
13. Iwasa S, Ikeda M, Okusaka T, Ueno H, Morizane C, Nakachi K, et al. Transcatheter arterial infusion chemotherapy with a fine-powder formulation of cisplatin for advanced hepatocellular carcinoma refractory to transcatheter arterial chemoembolization. Jpn J Clin Oncol. 2011;41:770–5.
14. Kirikoshi H, Yoneda M, Mawatari H, Fujita K, Imajo K, Kato S, et al. Is hepatic arterial infusion chemotherapy effective treatment for advanced hepatocellular carcinoma resistant to transarterial chemoembolization? World J Gastroenterol. 2012;18:1933–9.
15. Yoshikawa M, Ono N, Yodono H, Ichida T, Nakamura H. Phase II study of hepatic arterial infusion of a fine-powder formulation of cisplatin for advanced hepatocellular carcinoma. Hepatol Res. 2008;38:474–83.
16. Court WS, Order SE, Siegel JA, Johnson E, DeNittis AS, Principato R, et al. Remission and survival following monthly intraarterial cisplatinum in nonresectable hepatoma. Cancer Invest. 2002;20:613–25.
17. Ueshima K, Kudo M, Takita M, Nagai T, Tatsumi C, Ueda T, et al. Hepatic arterial infusion chemotherapy using low-dose 5-fluorouracil and cisplatin for advanced hepatocellular carcinoma. Oncology. 2010;78(Suppl 1):148–53.
18. Yamasaki T, Kimura T, Kurokawa F, Aoyama K, Ishikawa T, Tajima K, et al. Prognostic factors in patients with advanced hepatocellular carcinoma receiving hepatic arterial infusion chemotherapy. J Gastroenterol. 2005;40:70–8.
19. Obi S, Yoshida H, Toune R, Unuma T, Kanda M, Sato S, et al. Combination therapy of intraarterial 5-fluorouracil and systemic interferon-alpha for advanced hepatocellular carcinoma with portal venous invasion. Cancer. 2006;106:1990–7.
20. Uka K, Aikata H, Takaki S, Miki D, Kawaoka T, Jeong SC, et al. Pretreatment predictor of response, time to progression, and survival to intraarterial 5-fluorouracil/interferon combination therapy in patients with advanced hepatocellular carcinoma. J Gastroenterol. 2007;42:845–53.
21. Monden M, Sakon M, Sakata Y, Ueda Y, Hashimura E, FAIT Research Group. 5-Fluorouracil arterial infusion + interferon therapy for highly advanced hepatocellular carcinoma: a multicenter, randomized, phase II study. Hepatol Res. 2012;42:150–65.
22. Therasse P, Arbuck SG, Eisenhauer EA, Wanders J, Kaplan RS, Rubinstein L, et al. New guidelines to evaluate the response to treatment in solid tumors. European Organization for Research and Treatment of Cancer, National Cancer Institute of the United States, National Cancer Institute of Canada. J Natl Cancer Inst. 2000;92:205–16.